UDC 66.099

No of state registration 0119U100834

Inv. No

Ministry of Education and Science of Ukraine

Sumy State University

40007, Sumy, R.-Korsakova str., 2;

phone. (0542) 33-41-08/33-40-49

APPROVED

Vise-rector for scientific work

D.Sc. (physics and mathematics),

professor

_____ A.M. Chornous

REPORT

ON RESEARCH WORK

Small-scale energy-saving modules with the use of multifunctional devices with intensive hydrodynamics for the production, modification and encapsulation of granules

DEVELOPMENT AND CREATION OF TEST EQUIPMENT FOR THE PRODUCTION OF MONODISPERSE DROPLETS FROM SOLUTIONS AND MELTS WITH VIBRATING INFLUENCE ON THE MELT STREAM AND THE GRANULATION OF MINERAL FERTILIZERS IN THE VORTEX GAS STREAM, CARRYING OUT OF TESTING

(intermediate)

Manager of research work

Ph.D. (technical sciences), assoc. prof., senior researcher A.E. Artyukhov

2019

The manuscript was complete on December 24, 2019.

The results of this work were considered by the Scientific Council, Minutes from 2019.12.26 No. 6

LIST OF AUTHORS

Manager of research work Ph.D. (technical sciences)	A.E. Artyukhov (subsection 1.2, conclusions)
Responsible performer:	
Senior research officer Ph.D. (technical sciences)	N.O. Artyukhova (subsection 2.1)
Performers:	
Principal researcher D.Sc. (technical sciences)	V.I. Sklabinskiy (subsection 1.1)
Senior researcher Ph.D. (technical sciences)	R.O. Ostroha (subsection 2.2, part 1)
Senior researcher Ph.D. (technical sciences)	V.M. Kozin (subsection 2.2, part 2)
Junior researcher	A.V. Ivaniia (abstract)
Junior researcher	O.M. Gavrylenko (introduction)

ABSTRACT

Report on research work: 59 p., 27 figures, 3 tables, 13 references.

DIRECTIONAL MOTION OF THE FLUIDIZED BED, FREE AND CONSTRAINT MOTION, GRANULATOR, HYDRODYNAMIC OF FLOW MOVEMENT, JET DECAY, MELT DISPERSION PROCESS, NUMERICAL METHODS, OPTIMIZATION, ROTATING PERFORATED SHELL ACTIVE HYDRODYNAMIC REGIME, TRAJECTORY, VIBRATION.

Research object – hydrodynamic and heat-mass exchange characteristics of the target and supporting processes in the granulation modules with intensive hydrodynamics.

The aim of the research is a theoretical description and experimental study of the equipment for the production of monodisperse droplets from solutions and melts with vibrating influence on the melt stream and the granulation and drying of mineral fertilizers in the devices with active hydrodynamics.

Methodology. Mathematical modeling of hydrodynamic flows was carried out based on the points of classical fluid and gas mechanics and technical hydromechanics. Reliability of the obtained experimental results is based on the application of time-tested in practice methods.

Hydrodynamic properties of the liquid jet outflow were obtained. The presented mathematical model allows calculation of the radial component of the jet outflow velocity, as well as determination of the influences of physical and chemical properties of the liquid and the outflow hole diameter on the jet length and flow velocity along the axis to its disintegration into separated drops. The developed mathematical model extended with the theoretical description of the melt dispersion process from rotating perforated shells allowed us to improve design of the granulator to stabilize hydrodynamic parameters of the melt movement. The nitrogen fertilizers melt disperser

was investigated regarding industrial-scale production and operating parameters of the process of jet decay into drops, drop size and monodispersity level were optimized.

The results of the optimization calculation of devices with active hydrodynamics let to provide:

– a minimum “hydrodynamic” residence time of the particle in the device, which will not exceed “thermodynamic” time (minimum time of particles dehydration to the normative index is determined by the dehydration kinetics laws, thermodynamic indices of the dehydration process);

– implementation of different temperature and humidity potential of the heat transfer agent in some sections in the devices;

– variety of the device construction;

– possibility to use the recirculation of the heat transfer agent.

The original methods of the equipment engineering calculation with the directed fluidized bed as a part to obtain the granulated products are found.

The main recommendations to improve the technological equipment construction of the granulation unit have been implemented in the new methods of granulation and drying.

CONTENTS

INTRODUCTION

Report section "Introduction" is prepared in according to data [1].

Liquid dispersion processes forming micro- or macro drops are used in power generation, medicine, chemical industry, agriculture and other spheres of human activity. Efficiency of these technological processes and equipment is largely determined by the quality of liquid dispersion, which usually involves obtaining monodisperse drops.

This fully applies to the production of the commodity form of nitrogen fertilizers, which is carried out in two main ways:

– granulation starting from the liquid phase by dispersing it on the surface of suspended particles in a fluidized bed that can be variously configured (technologies of Casale S.A., Switzerland; Kahl Group, Germany; Stamicarbon, Netherlands; Toyo Engineering Corporation, Japan; Thyssenkrupp Fertilizer Technology GmbH, Germany, etc.), including vortex granulation;

– granulation starting from the liquid phase by dispersing into drops followed by crystallization of the solute by dewatering and cooling (prilling) (devices of Norsk Hydro, Norway; Didier Engineering GmbH, Germany; Imperial Chemical Industries, UK; Kaltenbach-Thuring S. A., France, etc.).

In these methods, among others, devices with different forms of a perforated shell, generally being axially symmetrical, can be used for dispersion of the nitrogen fertilizer melt.

Melt dispersion devices can be classified by the form of the working part (*i.e.* perforated shell) and by the presence of internal devices in the perforated shell. Additionally, these devices differ in the nature of force acting on the melt and can be static, swirl (tangential introduction of the melt into a perforated shell or to the turbine for the melt spin), and dynamic (rotating).

In recent years, preference is mainly given to conical or cylindrical rotating devices and devices with the cup-shaped shell. This is due to simplicity of operation and high

uniformity of resulting liquid drops and commodity granules in comparison to analogue devices. For example, ammonium nitrate granulators (dispersers), which are currently in operation, provide manufacturing of products with following granulometric composition in terms of mass fraction: 0.5 - 1.5 % of granules < 1.0 mm in size, 90 – 98 % of granules in the size range 2.0 - 4.0 mm, where granules in the size range 2.0 - 2.5 mm comprise 42 – 71 % and granules in the size range 2.0 - 3.0 mm comprise 85 - 95 %. Dispersion of melts producing more than 2 % of dust-forming particles of less than 1.0 mm as well as those over 3.5 mm in size, which can be also destructed making dust, leads to dust formation of nitrogenous fertilizers in air in the tower.

In existing equipment, calculation of hydrodynamic characteristics of the liquid jet that is dispersed, is often not performed, resulting in sub-optimal uniformity of the obtained drops. Hydrodynamic parameters of the liquid jet issuing from a single hole or holes of the perforated shell, and design features of devices for fluid dispersion influence the process of jet decay into drops.

The problem of creating the adequate model of jet decay into drops at the opening in a thin wall is highly relevant for dispersion improvement in granulation devices in the mineral fertilizers production. By controlling the jet decay process, we can optimize performance of the disperser and create favourable conditions to produce a product with a high degree of monodispersity.

1 RESEARCH OF THE EQUIPMENT FOR THE PRODUCTION OF MONODISPERSE DROPLETS FROM SOLUTIONS AND MELTS WITH VIBRATING INFLUENCE ON THE MELT STREAM

1.1 Decay of the melt stream during dispersion

This report section is prepared in according to data [1].

Experimental rotating vibration granulator

A rotating vibration granulator is the main unit of the experimental system (figure 1), which consists of a variable perforated membrane 1 with holes to discharge the fluid, housing 2 with a distributive drive 3 and a pipe 4 for introducing air from the fan 5. The housing 2 is also supplied with a fixed liquid distributor 6 with a pipe 7 and a filter element 8.

At the top of the fluid atomizer, a mechanical, electrical or electromagnetic vibrator 9 is installed, which is connected by a rod 10 with the resonator 11 in the form of an elastic disc or plate.

When the granulator is working, liquid that goes through the pipe 7 and the distributor 6 to the bottom part of the granulator flows out of the holes of the perforated membrane. Simultaneously, air at a given pressure is supplied by the fan 5 through the pipe 4 into the cavity of the granulator.

The installation is equipped with a buffer bunker 12 for liquid with a circulation pump 13. Valve 14 and rotameter 15 are used to regulate and measure the liquid flowrate. The oscillations sensor 16 is connected with an oscillograph 17 to observe fluctuations while the digital frequency meter 18 is used to measure the oscillation frequency. When the electrodynamic or electromagnetic vibrator is used, regulation of oscillations is carried out by the electronic controller 19. A stroboscope (20 and 21) is installed for visual observation of the process of liquid dispersion into drops. Measurements of the liquid pressure in holes and air at the free surface of the liquid are carried out by manometers 22 and 23, respectively. The controller 24 is aimed to regulate the air pressure in the granulator.

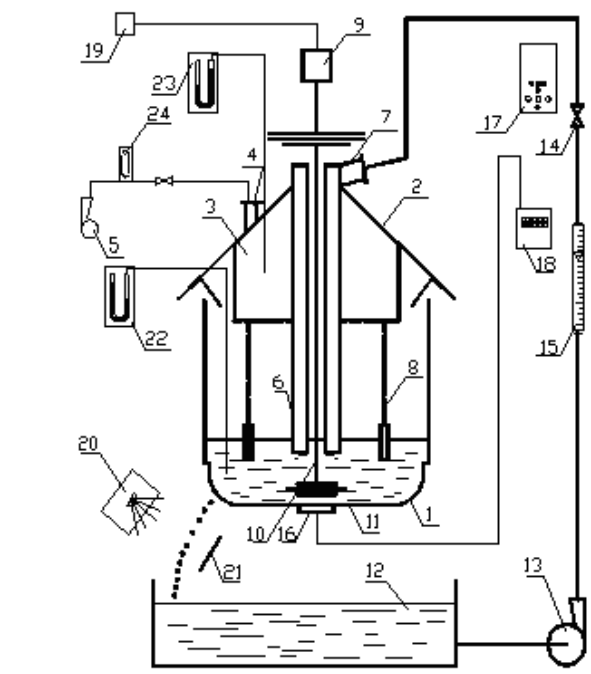

a

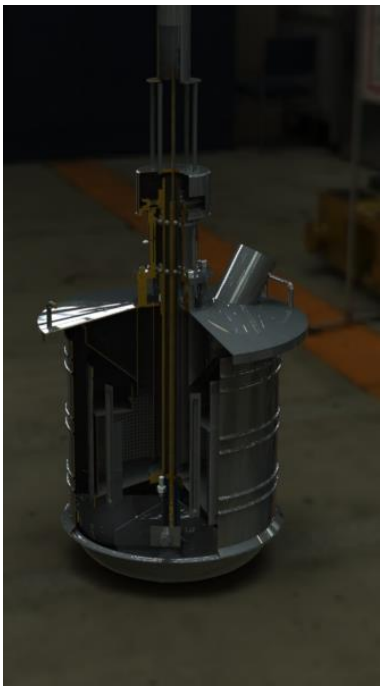

b

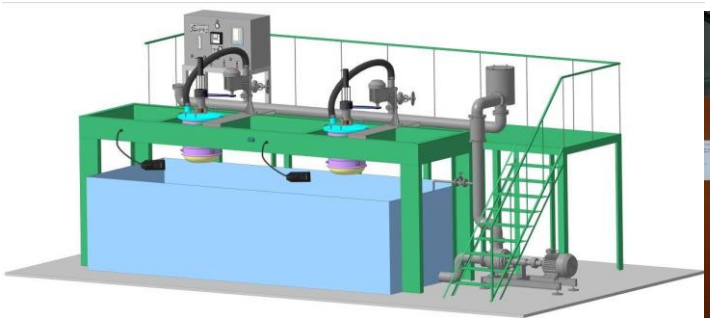

c

Figure 1 – Experimental installation of the rotating vibration granulator: a) a schematic presentation of the granulator: 1- perforated membrane (diameters of holes are 1.0 mm, 1.1 mm, 1.2 mm, 1,3mm, 1,4 mm, number of holes is 1800-2300, bottom shape is toroidal, length is 650 mm, diameter is 560 mm), 2 – housing (height is 590 mm, diameter is 560 mm), 3 – distributive drive, 4 – pipe (diameter is 45 mm), 5 – fan, 6 – liquid distributor, 7 – pipe (diameter is 100 mm), 8 - filter element (metal grid), 9 – vibrator (MFR OTY 77 actuator, range of output frequency 120-1200 is Hz), 10 – rod, 11 - resonator, 12 - buffer bunker, 13 – circulation pump (model Calpeda NC3 25-50/180), 14 – valve, 15 – rotameter (model Raifil RF FM 10), 16 - oscillations sensor, 17 – oscillograph (model C1-65A), 18 – digital frequency meter (model VC3165), 19 – electronic controller, 20, 21 – elements of stroboscope, 22, 23 – manometers (model МТ-2У), 24 – controller (model Euroaqua SKD-1); b) 3D model of the vibrating granulator; c) 3D model and a photograph of the experimental installation

Next, the electronic oscillator 19 is switched on and the electrodynamic vibrator 9 started resulting in vibration of the resonator at a certain frequency, which is fixed and recorded by the digital frequency meter 18, which is connected to the vibration sensor 16 of the granulator basket. Air is supplied into the granulator by turning the fan 5 on, and when the interstitial position is changed, the certain pressure is installed based on manometer data. The process of jets dispersion into drops is simultaneously monitored by using a stroboscope 20. When formation of monodisperse drops (without satellite droplets) is observed, measurements are recorded at the manometer 22, which corresponds to the total liquid pressure in the leakage holes, and at the digital frequency meter 18 showing the vibration frequency (upper limit). These liquid and air parameters are varied by changing the vibration frequency by the electronic generator 19 at the lower limit of the granulator stable operation range. Ranges of stable operation are determined for different liquid leakage velocities from holes in the basket, which can be achieved by changing the granulator performance under the constant air pressure or by changing the air pressure by using the pressure regulator at the constant granulator performance. When operating the rotating vibration granulator at different liquid leakage velocities, the fluid flow rate is measured by a graduated cylinder.

Physical modeling is based on methods of the similarity theory. The geometric similarity is maintained by equality of appropriate constants and invariants.

The special frequency generator is designed to generate vibration on the radiator of the rotating vibration melting granulator by feeding electric signals of a special shape on the MFR OTY 77 actuator.

Processing of the experimental results

Velocity, V, of the liquid leaking from the granulator holes is calculated as:

$$V = \phi\sqrt{2gH} \tag{1}$$

where φ is the discharge coefficient and set to 0.96-0.98.

According to experimental data of upper f_1 and lower f_2 limits of the frequency, which provide a monodisperse liquid jet decay, the maximum and minimum lengths of the wave are calculated:

$$\lambda_{max} = V/f_1;\ \lambda_{min} = V/f_2 \tag{2}$$

The melt flowrate, G_S, through the granulator hole is calculated from the measured leaked melt volume, G_τ and time, τ:

$$G_s = G_\tau/\tau \tag{3}$$

Diameter of drops, formed by the decay of liquid jets at the average vibration frequency of the granulator, f_{avi}, is determined from the material balance according to the equation:

$$d_{dr} = \sqrt[3]{\frac{6G_s}{\pi f_{avi}}} \tag{4}$$

The absolute difference of drop diameters and a relative deviation of drop diameters from the average drop diameter at the granulator maximum and minimum productivity are calculated as follows:

$$\Delta d_{dr}^{ab} = d_{dr}^{max} - d_{dr}^{min} \tag{5}$$

$$\Delta d_{dr}^{rel} = \frac{2(d_{dr}^{max} - d_{dr}^{min})}{d_{dr}^{max} + d_{dr}^{min}} \tag{6}$$

To define the optimal number of experiments and the highest accuracy degree and reliability of the obtained results, as well as for the processing of these results, methods of mathematical statistics were used.

Theoretical model

The model of the jet decay is based on the solution of Navier-Stokes equations (7) - (8) and the flow continuity equation (9) in cylindrical coordinates [9], with the following simplifications:

– flow is axially symmetrical;

– cross-section of the jet is circular, there is only jet restriction and extension (the tangential component of jet velocity υ_θ=0).

$$\upsilon_r \frac{\partial \upsilon_r}{\partial r} = -\frac{1}{\rho}\frac{\partial p}{\partial r} + v\left[\frac{\partial^2 \upsilon_r}{\partial z^2} + \frac{\partial}{\partial r}\left(\frac{\frac{\partial}{\partial r}(r\upsilon_r)}{r}\right)\right] \tag{7}$$

$$\upsilon_z \frac{\partial \upsilon_z}{\partial z} = -\frac{1}{\rho}\frac{\partial p}{\partial z} + v\left[\frac{\partial^2 \upsilon_z}{\partial z^2} + \frac{1}{r}\frac{\partial}{\partial r}\left(r\frac{\partial \upsilon_z}{\partial r}\right)\right] \tag{8}$$

$$\frac{\partial \upsilon_z}{\partial z} + \frac{1}{r}\frac{\partial}{\partial r} r\upsilon_r = 0 \tag{9}$$

By assuming that the axial velocity component at the time of leaving the hole varies parabolically with the radial coordinate:

$$\upsilon_z = A_1 r^2 z^2 + A_2 r + A_3 \tag{10}$$

And transforming the equation (9), we obtain the value of the radial component of the jet velocity:

$$\upsilon_r = \frac{-\frac{1}{2}A_1 r^4 z + F_1(z)}{r} \tag{11}$$

where $F_1(z)$ is a polynomial function.

Given the fact that the pressure change in a jet in the radial direction is insignificant compared to the axial component, and by substituting (10) into (8) we get:

$$2\left(A_1 r^2 z^2 + A_2 r + A_3\right) A_1 r^2 z = \frac{1}{\rho}\frac{dp}{dz} + \nu\left(2A_1 r^2 + \frac{4A_1 r z^2 + A_2}{r}\right) \tag{12}$$

By solving the equation (12) for dp/dz and by integration the expression for pressure change along the jet axis it is obtained:

$$p(z) = -\frac{1}{r}\left(\frac{1}{3}\rho\left(\frac{1}{2}A_1^2 r^5 z^4 + A_1 r^4 z^2 A_2 + A_1 r^3 z^2 A_3 - 2\nu A_1 r^3 z - \frac{4}{3}\nu A_1 r z^3 - \nu A_2 z\right)\right) + C_1 \tag{13}$$

By setting the origin of the coordinate system at the hole exit (z = 0) and by introducing the assumption that the liquid outflow occurs at a constant pressure (p = const), then according to (13) it is obtained that $C_1 = p_1$.

After insertion of this constant we get:

$$p(z) = -\frac{1}{r}\left(\frac{1}{3}\rho\left(\frac{1}{2}A_1^2 r^5 z^4 + A_1 r^4 z^2 A_2 + A_1 r^3 z^2 A_3 - 2\nu A_1 r^3 z - \frac{4}{3}\nu A_1 r z^3 - \nu A_2 z\right)\right) + p_1 \tag{14}$$

By inserting (14) into (7) we obtain the differential equation of total derivatives in respect to the function $F_1(z)$:

$$\frac{\left(-\frac{1}{2}A_1r^4z+F_1(z)\right)\left(-2A_1r^2z-\frac{-\frac{1}{2}A_1r^4z+F_1(z)}{r^2}\right)}{r}=-\frac{1}{\rho}\left(\frac{1}{2}\rho\right)A_1^2r^5z^4+A_1r^4z^2A_2+$$

$$+A_1r^3z^2A_3-2\nu A_1r^3z-\frac{4}{3}\nu A_1rz^3-\nu A_2z\left(-\frac{1}{r}\right)-\left(\frac{1}{2}\rho\right)r^4A_1^2z^4+4A_1r^3z^2A_2+$$

$$+3A_1r^2z^2A_3-6\nu A_1r^2z-\frac{4}{3}\nu A_1z^3+\nu\left(\frac{1}{r}\right)\frac{d^2F_1(z)}{dz^2}-4A_1rz \tag{15}$$

Based on the fact, that the derivative $d\upsilon_r/dz$ is equal to:

$$\frac{d\upsilon_r}{dz}=\frac{-\frac{1}{2}A_1r^4z+\frac{dF_1(z)}{dz}}{r} \tag{16}$$

And the radial velocity component of the jet at z=0 becomes $\upsilon_r=0$, we obtain:

$$\frac{1}{2}A_1r^4z=\frac{dF_1(z)}{dz}. \tag{17}$$

By using the boundary conditions $F_1(z=0)=0$ and $dF_1/dz\ (z=0)=0$, and putting them into the equation (10) we obtain the value of the function F_1 as a polynomial:

$$F_1(z)=\frac{(-A_2+8A_1r^3)z^3}{6r}+\frac{A_1r^2(3A_1r^4-12A_2r-8A_3)z^4}{48\nu}. \tag{18}$$

Substituting the relation (18) in the equation (11) leads to:

$$\upsilon_r=\frac{z\left(24A_1r^5\nu-8\nu z^2A_2+64\nu z^2A_1r^3+3A_1^2r^7z^3-12A_1r^4z^3A_2-8A_1r^3z^3A_3\right)}{48\nu r^2}. \tag{19}$$

The coefficient A_2 can be found by assuming that on the jet surface $r=r_s$ the pressure p is equal to the pressure of the surrounding environment p_0. This boundary condition can be written as:

$$p_0 = -\frac{1}{r_s}\left(\frac{1}{3}\rho\left(\frac{1}{2}A_1^2 r_s^5 z^4 + A_1 r_s^4 z^2 A_2 + A_1 r_s^3 z^2 A_3 - 2\nu A_1 r_s^3 - \frac{4}{3}\nu A_1 r_s z^3 - \nu A_2 z\right)\right) + p_1 \qquad (20)$$

Thus, the coefficient A_2 is now calculated as:

$$A_2 = -\frac{(r_s(3z^4 A_1^2 \rho r_s^4 + 6z^2 A_1 \rho r_s^2 A_3 - 12zA_1\rho\nu r_s^2 - 8\rho\nu A_1 z^3 - 6p_1 + 6p_0))}{6\rho z(A_1 r_s^4 z - \nu)}. \qquad (21)$$

The coefficient A_3 can be defined by assuming that that if $r=0$, $\upsilon_r=0$:

$$A_3 = -\frac{3z^4 A_1^2 \rho r_s^4 + 6p_0 - 12zA_1\rho\nu r_s^2 - 8\rho\nu A_1 z^3 - 6p_1}{6z^2 r_s^2 \rho A_1}. \qquad (22)$$

Accordingly,

$$\upsilon_z = A_1 r^2 z^2 - \frac{3z^4 A_1^2 \rho r_s^4 + 6p_0 - 12zA_1\rho\nu r_s^2 - 8\rho\nu A_1 z^3 - 6p_1}{6z^2 r_s^2 \rho A_1}. \qquad (23)$$

The coefficient A_1 is determined by assuming that at a point close to the origin of the coordinate system $z = z_0$, the exhaust velocity has not yet changed its value and is equal to the flow velocity jet in the hole $\upsilon_z = \upsilon_{z0}$ that is:

$$\upsilon_{z_0} = \frac{6A_1^2 r^2 z_0^4 r_s^2 - 3z_0^4 A_1^2 \rho r_s^4 - 6p_0 - 12z_0 A_1\rho\nu r_s^2 + 8\rho\nu A_1 z_0^3 + 6p_1}{6z_0^2 r_s^2 \rho A_1}. \qquad (24)$$

When we solve the resulting equation (24) for the coefficient A_1, we obtain:

$$A_1 = \frac{1}{3z_0^3 r_s^2 \rho(2r^2 - r_s^2)}(-4\nu\rho z_0^2 + 3\upsilon_{z0} r_s^2 \rho z_0 - 6\rho\nu r_s^2 + (16\nu^2\rho^2 z_0^4 -$$

$$-24\nu\rho^2 z_0^3 \upsilon_{z0} r_s^2 + 48\nu^2\rho^2 z_0^2 r_s^2 + 9\upsilon_{z0}^2 r_s^4 \rho^2 z_0^2 - 36\upsilon_{z0} r_s^4 \rho^2 z_0 \nu + 36\rho^2\nu^2 r_s^4 +$$

$$36z_0^2 r^2 r_s^2 \rho p_0 - 36z_0^2 r^2 r_s^2 \rho p_0 - 36z_0^2 r^2 r_s^2 \rho p_1 - 18z_0^2 r_s^4 \rho p_0 + 18z_0^2 r_s^4 \rho p_1)^{1/2}) \qquad (25)$$

The presented mathematical model allows calculating radial and axial components of the velocity jet outflow, as well as to establish the influence of physical and chemical properties of the liquid and the hole diameter on the jet length and velocity along the axis to its disintegration into separate drops (figures 2, 3).

The radial component of the velocity scarcely appears at a short distance from the hole. When the distance increases, radial flows in the jet appear, which cause its breaking-up into drops. It is indicated by the significant increase of the radial component. Increases in the temperature of the melt and the diameter of the perforated shell hole lead to the reduction of the distance from the hole, at which the radial component becomes critical that is at which the jet is broken up. The negative velocity indicates the break off of the flow (detachment of the jet with the formation of the vortex flows), which disappears with an increase of parameter z.

The smaller the distance from the outflow hole during jet breaking-up, the smaller the length of the jet portion, which forms the drop volume during jet breaking-up. This hypothesis coincides with the results of other scientists' studies.

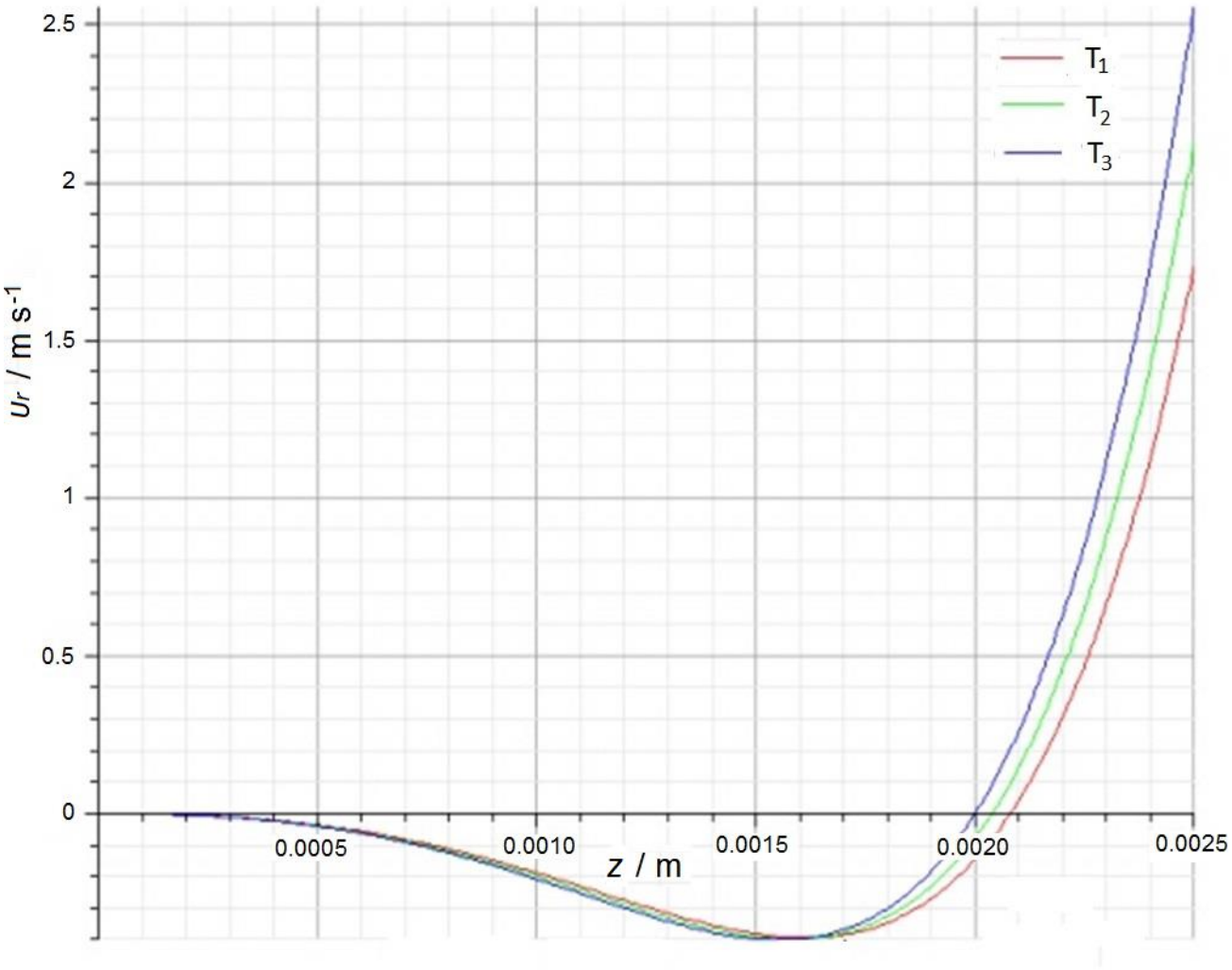

Figure 2 – Dependence of the radial component of the jet velocity of the ammonium nitrate melt on the axial distance, z, from the hole 1.3 mm in diameter at different temperatures of the melt at T_1 = 175°C, T_2 =180°C, T_3 = 185°C and the vibration frequency of 340 Hz (viscosities were 5.36, 5.03, 4.74 mPa·s, densities were 1434, 1431, 1428 kg/m^3 respectively)

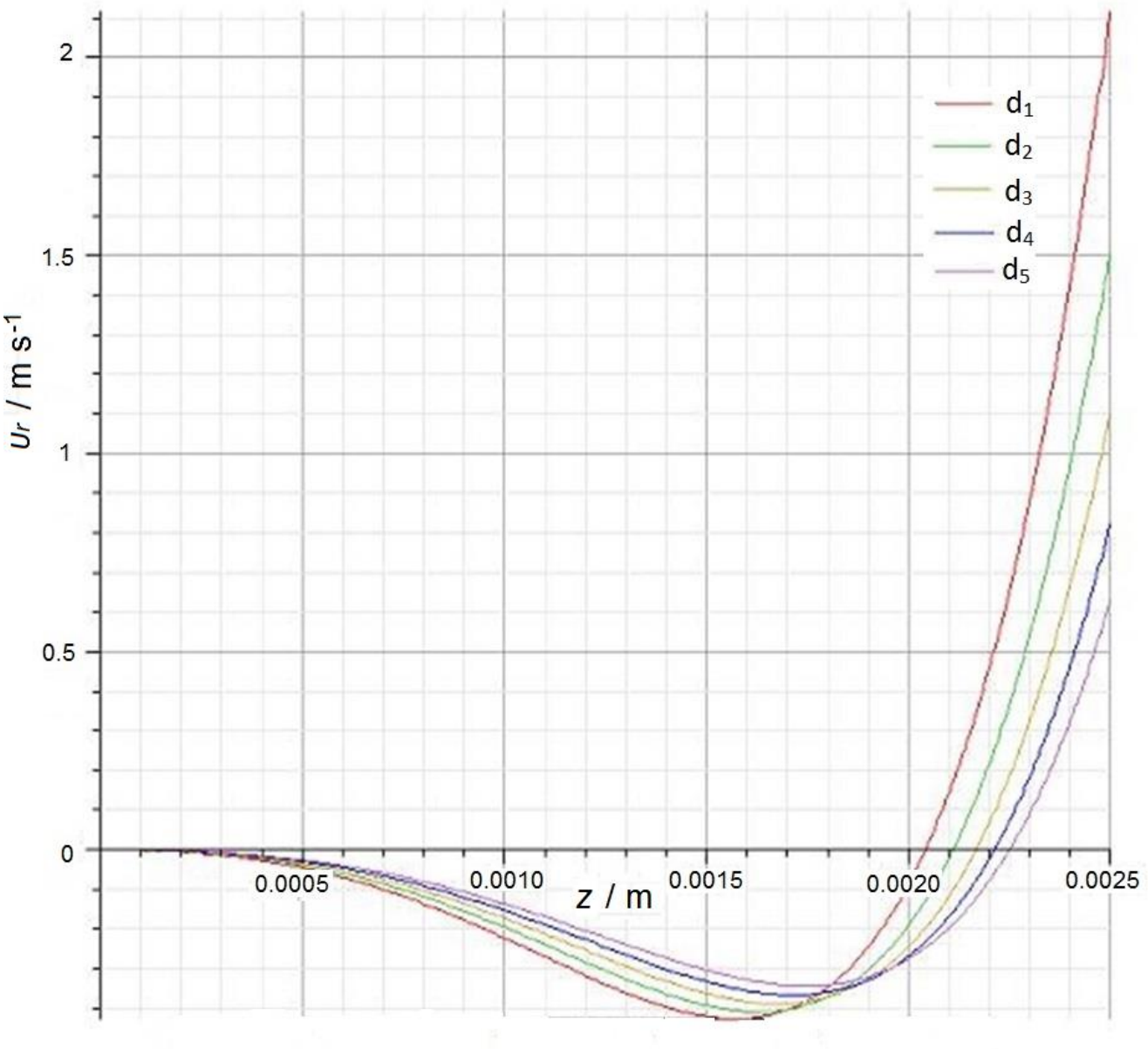

Figure 3 – Dependence of the radial component of the jet velocity of the ammonium nitrate melt on the axial distance, z, from the holes of different diameters: d_1=1.0 mm, d_2=1.1 mm, d_3=1.2 mm, d_4=1,3mm, d_5=1,4 mm at the temperature of 185°C (viscosity was 4.74 mPa·s, density was 1428 kg/m^3) and the vibration frequency of 340 Hz

For the granulator basket rotation velocity of n = 60 rpm and a load of 37 t/h optimal diameter of the hole is d = 1.2 mm and the melt temperature is 185 °C.

An example of comparison of theoretical calculations and experimental results of velocity radial component measurement is shown in table 1.

Table 1 – An example of comparison of theoretical calculations and experimental results of υ_r measurement (hole diameter was 1.3 mm, temperatures of the melt was 175°C (viscosity was 5.36 mPa·s, density was 1434 kg/m^3), vibration frequency was 340 Hz, granulator basket rotation velocity was n = 60 rpm and a load was 37 t/h**)**

$\upsilon_{r.theor}$ / m s^{-1}	No of measurement	$\upsilon_{r.exp}$ / m s^{-1}	$\upsilon_{r.theor}$ / m s^{-1}	No of measurement	$\upsilon_{r.exp}$ / m s^{-1}
z = 0 m			z= 0.0005 m		
0	1	0	-0.05	1	-0.04
0	2	-0.003	-0.05	2	-0.02
0	3	0.002	-0.05	3	-0.08
0	4	0	-0.05	4	-0.07
0	5	0.004	-0.05	5	-0.09
0	6	-0.005	-0.05	6	-0.04
z = 0.001 m			z = 0.0015 m		
-0.2	1	-0.21	-0.4	1	-0.4
-0.2	2	-0.19	-0.4	2	-0.42
-0.2	3	-0.19	-0.4	3	-0.39
-0.2	4	-0.19	-0.4	4	-0.38
-0.2	5	-0.18	-0.4	5	-0.4
-0.2	6	-0.2	-0.4	6	-0.41
z = 0.002 m			z = 0.0025 m		
0	1	-0.01	2.5	1	2.44
0	2	0.01	2.5	2	2.53
0	3	0.02	2.5	3	2.51
0	4	0	2.5	4	2.41
0	5	-0.03	2.5	5	2.56
0	6	0	2.5	6	2.6

Basket tests of the granulator confirmed the theoretical research and provided a basis for modernization of the equipment construction. During the tests, a stable jet breakup into drops at a distance of 2-5 mm from the wall of the perforated shell was obtained (figures 4, 5).

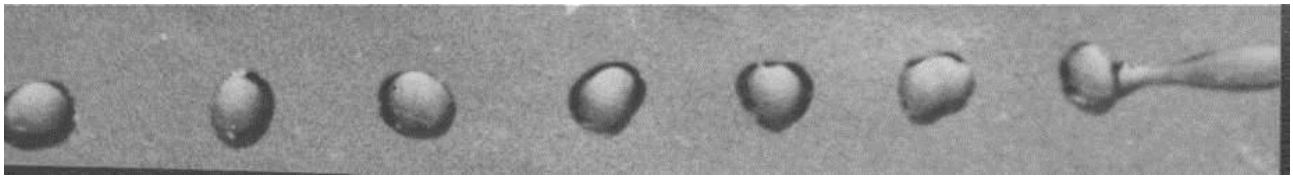

a

b

Figure 4 – Jet disintegration into drops after the outflow from the perforated shell: a) ammonium nitrate drops, vibration frequency of 200 Hz; b) ammonium nitrate drops, vibration frequency of 340 Hz. Diameter of the hole was 1.1 mm and the temperature was 185°C (viscosity was 4.74 mPa·s, density was 1428 kg/m^3). Granulator basket rotation velocity was n = 60 rpm and a load of 37 t/h

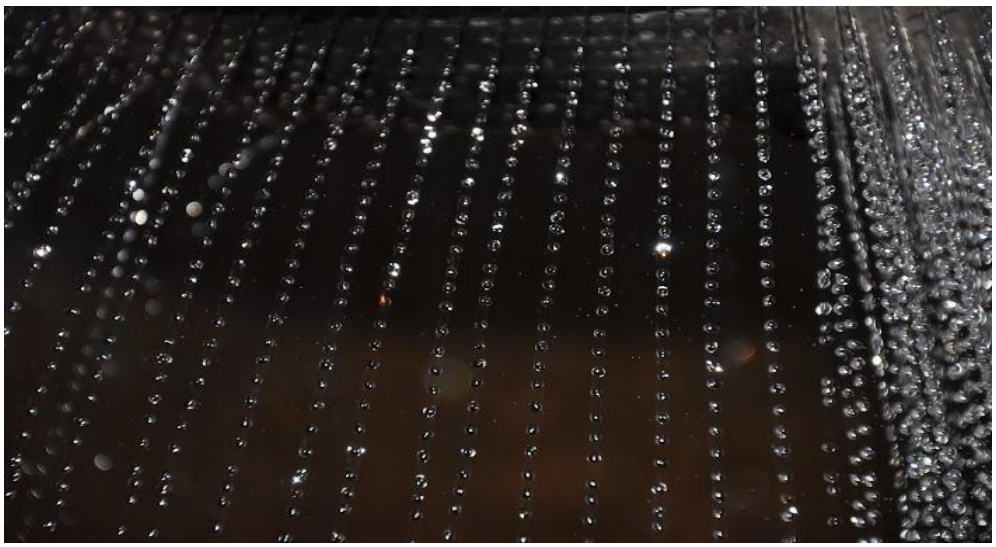

Figure 5 – Steady jet disintegration into drops after the outflow from the perforated shell: ammonium nitrate drops, vibration frequency of 340 Hz. Diameter of the hole was 1.1 mm and the temperature was 185°C (viscosity was 4.74 mPa·s, density was 1428 kg/m^3). Granulator basket rotation velocity was n = 60 rpm and a load of 37 t/h

The developed mathematical model was extended with the theoretical description of the melt dispersion process from rotating perforated shells, which allowed us to improve the granulator design to stabilize hydrodynamic parameters of the melt movement within it. By applying of a weighted vortex layer in combination with the vibrating material liquid spray and rotation of liquid jets by their decay should further improve the quality of the granulated product.

A scheme of the modernized granulator is shown in figure 6, and layout solutions for the granulator installation in a granulation tower in figure 7. Similarity of respective particles movements and their trajectories in the industrial design and in the experimental granulator is maintained.

The improved granulator has a guiding element in the form of an auger installed, so when the melt contacts the shoulder blade, the total melt pressure is increased by transforming the screw mechanical energy into the melt kinetic energy and then turning it into the internal energy. Possibility of screw rotation provides an option for increasing the pressure in front of the outflow holes.

Pilot testing of the improved granulator of the total capacity of 37 t/h in production of ammonium nitrate at different climatic conditions (humid and hot climate, temperate continental climate) showed a high yield of marketable fractions and reduction of dust content in flue gases. High level of monodispersity of granules is achieved by improving the fusion hydrodynamics in the granulator and by applying vibration to the jets leaking from the basket perforated bottom. Also the improved granulator significantly reduced the dust level in the air leaving the tower. Axial flow fans capture from 16 to 38 mg/m^3 of dust so that the granulator enables reduction of costs needed for purchasing expensive new equipment for treatment of the exhaust air.

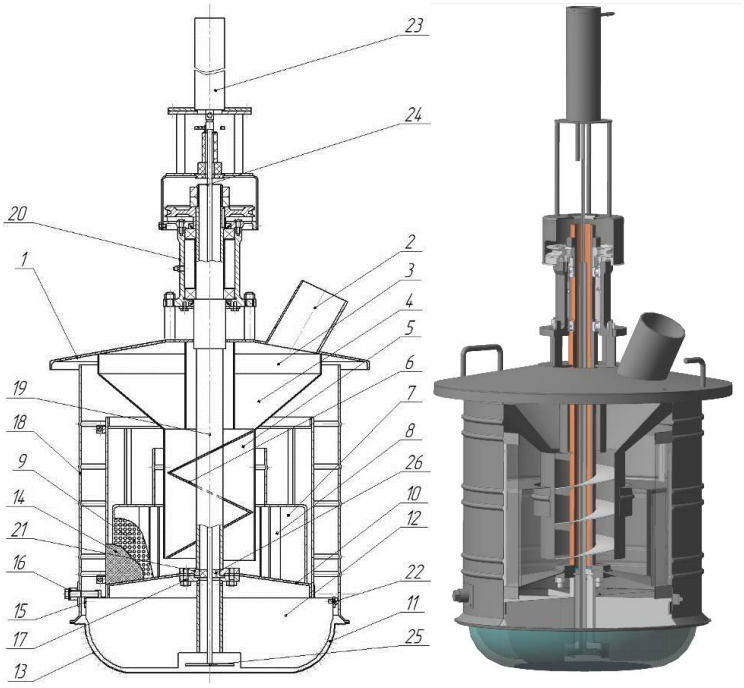

Figure 6 – The improved rotating vibration granulator of solutions (melts): 1 - housing; 2 - pipe for introducing the solution (melt); 3 - ring collector; 4 - reverse cone; 5 - annular channel; 6 - auger; 7 - distributor of the solution (melt); 8 - directing blades; 9 - perforated cylinder; 10 - directing cone for the solution (melt); 11 - perforated bottom (basket); 12 - pressure blades; 13 - hole; 14 - mesh for the final melt filtration; 15 - ring; 16 - bolts; 17 - pins; 18 - cylindrical chamber; 19 - hollow shaft; 20 - bearing assembly; 21 - flange connection; 22 - bulge for centering the cylindrical chamber; 23 - vibration device; 24 - rod; 25 - disc radiant; 26 - hub

Results of basic tests of the improved granulator are shown in figures 8 and 9. Analysis of figures 8 and 9 provides determination of an optimal (operating) vibration frequency (frequency range), at which the maximal degree of drop monodispersity is achieved. At these conditions, the melt jet disintegrates evenly and without formation of drop satellites.

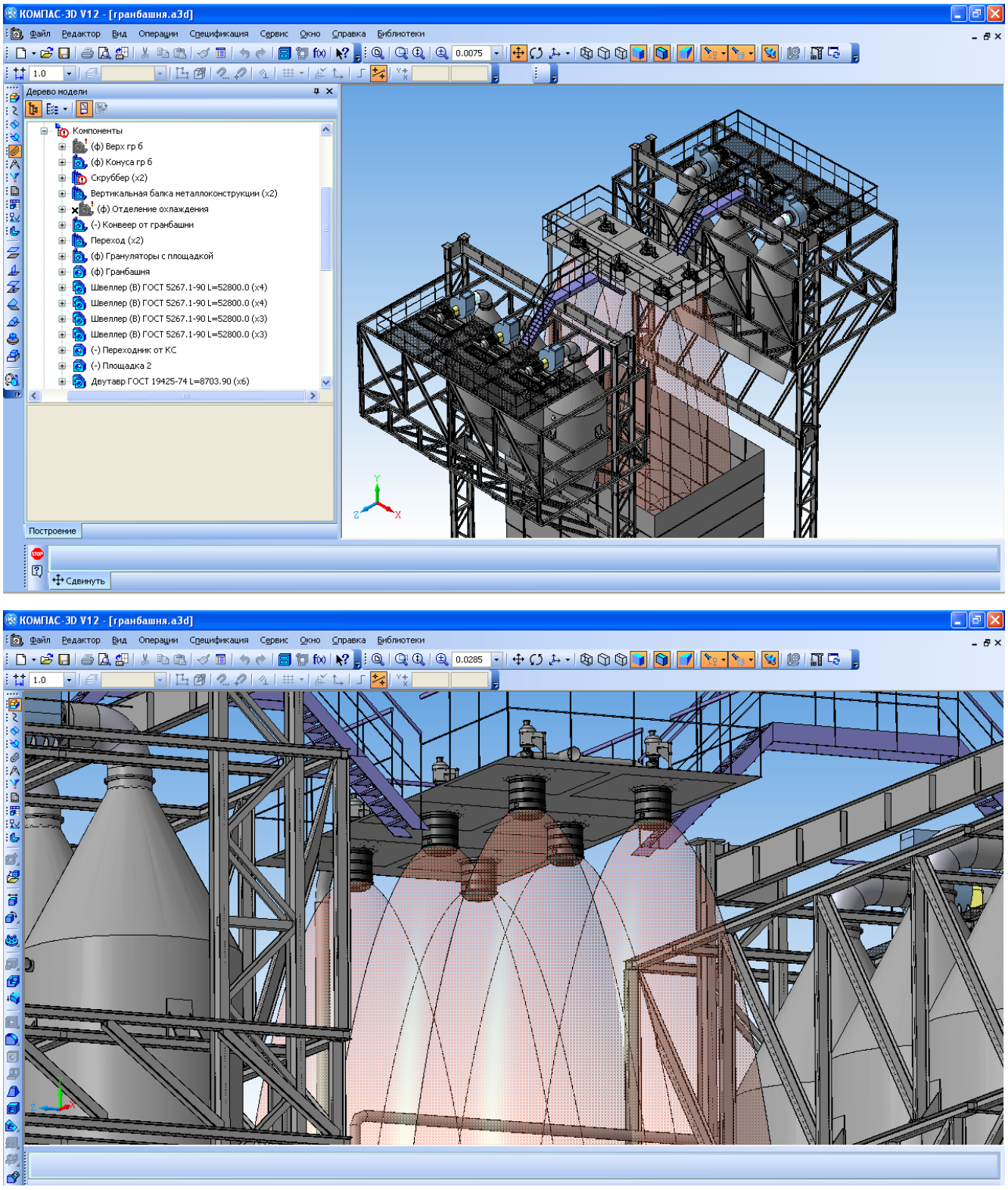

Figure 7 – Layout solutions for granulator installation in a granulation tower

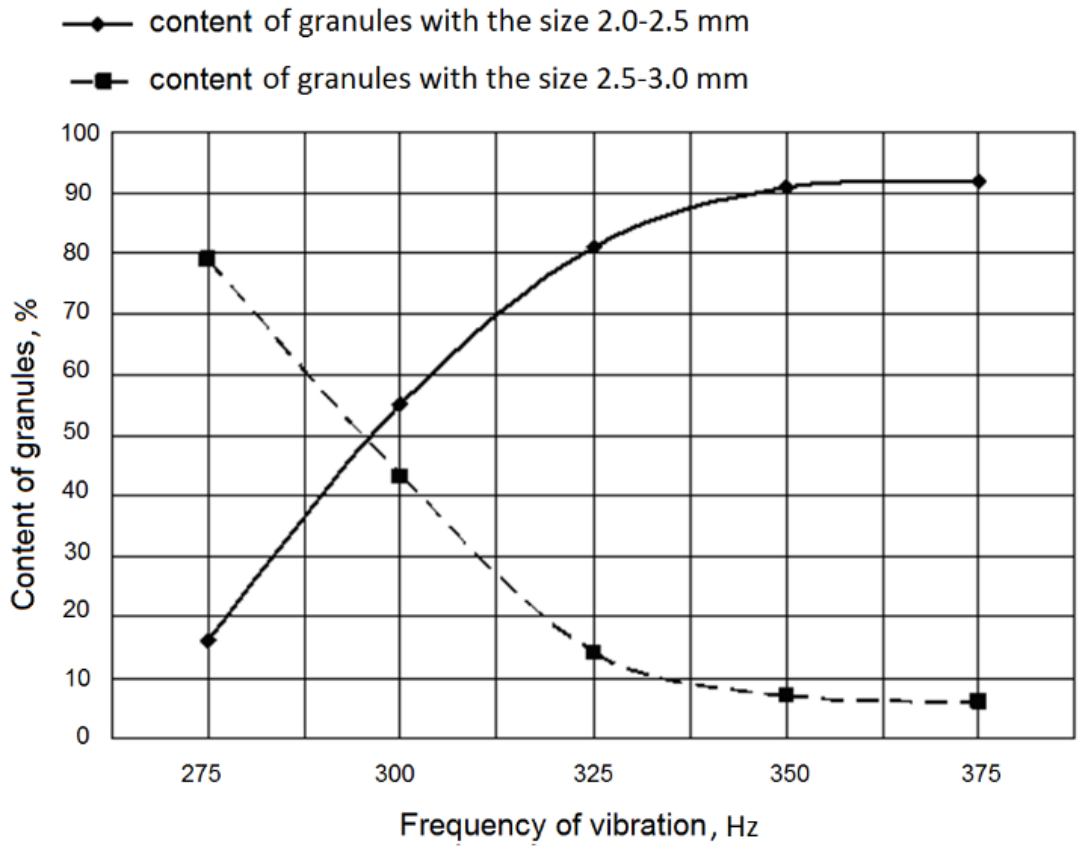

Figure 8 – Mass fractions of ammonium nitrate granules with sizes 2.0 – 2.5 mm and 2.5 - 3.0 mm as functions of the vibration frequency at the granulator basket rotation velocity of n = 60 rpm, load of 37 t/h and 1.2 mm hole diameter

The monodispersion process introduces a fundamental improvement in the fertilizer production technology. Use of uniform (monodisperse) granules, for example in agriculture, provides even distribution of the fertilizer on the fertilized area resulting in additional yields up to 10 % [10-12].

Vibrating granulators provide production of strong monodisperse granules with a smooth glossy surface (the monodispersity degree is up to 99 %). Thus, these devices open possibilities to intensify the granulation process and essentially improve the agrotechnical value of fertilizers.

Table 2 shows a comparative analysis of granulometric compositions of final products obtained in different types of granulators.

Table 2 – Comparison of granulometric content of products obtained in the improved rotating vibration granulator and in world analogues of the granulation equipment

Granule size range, mm	Granulometric content of products, %		
	Centrifugal granulator, company "Kreber" (Netherlands) [2]	Acoustics granulator designed by Research Institute at the Chemical plant (Russia) [3]	Improved rotating vibration granulator
1 - 4	97-99	98-99	more than 99
2 - 4	83-92	85-95	90-97
2 - 3	75-90	80-90	more than 90
2.0 - 2.5	40-50	45-65	more than 80
less than 1	0.8-2.5	0.8-1.5	0.1-0.8

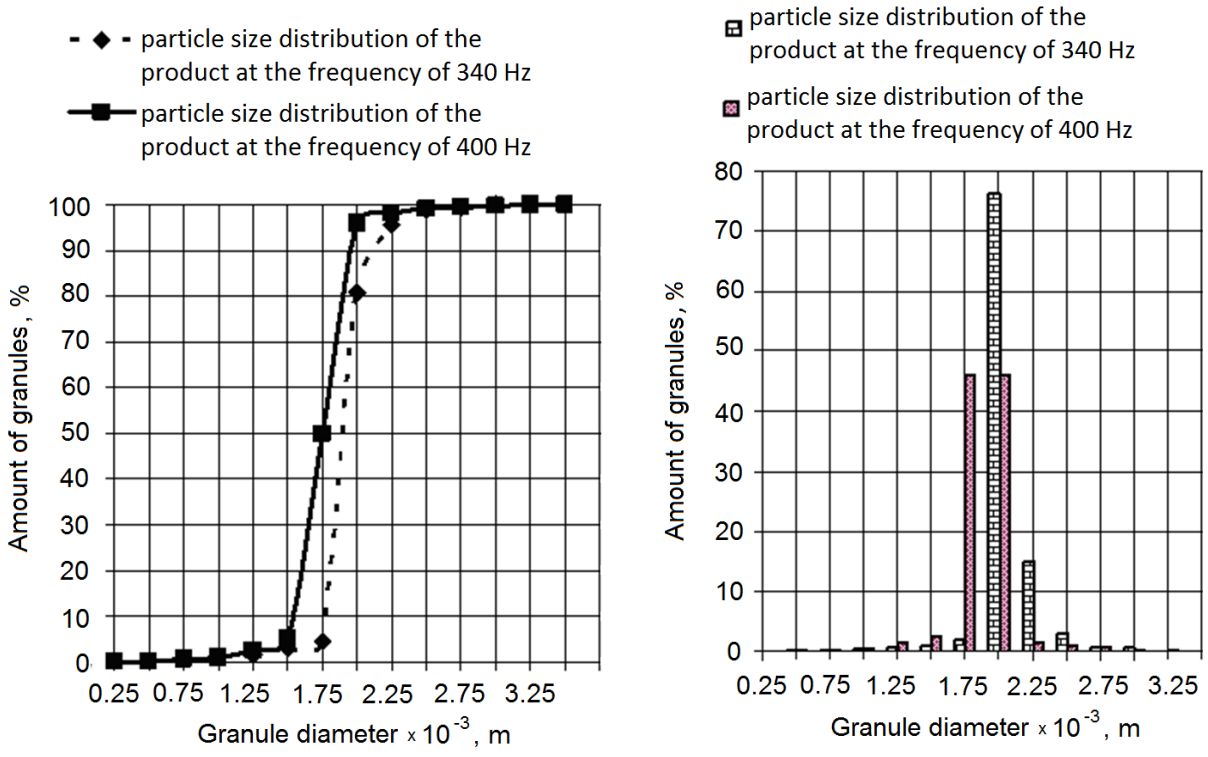

a b

Figure 9 – The integral particle size distribution of ammonium nitrate granules at vibration frequencies of 340 and 400 Hz and the granulator basket rotation velocity of n = 60 rpm, load of 37 t/h and the hole diameter of 1.2 mm: a) line graph b) bar chart

The improved granulator has following advantages over other granulator types:

- high safety in operation;
- production of more competitive uniform granules;
- avoidance of product's sticking in towers;
- decrease of dust;
- increase of the agro-technical value of fertilizers.

The improved vibrating granulators have a reliable vibration system, which provides a stable imposition of oscillations on fluid jets flowing out of perforated shell holes, regardless the changes in the load on the melt disperser. This vibration system provides measurements of the level of melt in the granulator and thereby, control of the clogging degree and melt outflow velocity from the holes of the perforated shell.

The improved vibrating granulator (figure 6) with an electromagnetic vibration system (vibration frequency of 340 Hz) provided production of a product with the following granulometric composition as mass fractions: 0.02 - 0.2 % of granules < 1.0 mm and over 96 % of granules 2.0 - 4.0 mm in size. Also, the fraction of granules in the size range 2.0 - 2.5 mm was not lower than 88 % with the main size in the range 2.1 - 2.5 mm. When the vibration frequency was changed to 400 Hz, the granulator provided a product with the main granule fraction (over 65 %) in the size range 2.5 - 3.0 mm with a simultaneously obtained increased granule hardness.

Similar granulometric compositions of products were obtained by using vibrating granulators with electromagnetic vibration systems in the ammonium nitrate production at tropical conditions in Cuba and in urea production with hydrohumates as foaming additives. During the industrial operation over one month the product (urea) was stably obtained with the following granulometric composition in mass fractions: 0.1 - 0.3 % of granules < 1.0 mm, 99.7 - 99.9 % of granules in the size range 1.0 - 4.0 mm where granules in the size range 2.0 - 4.0 mm comprised 96.5 - 98.9 % while granules larger than 4.0 mm were absent.

Consideration of hydrodynamic parameters of the liquid jet flowing out of holes of a perforated membrane allowed us to affect the process of jet decay into drops and

resulting drop size and dispersity and consequently to improve the construction of nitrogen fertilizers melt granulator.

Main results:

– a mathematical model was derived to calculate hydrodynamic properties of the melt jet expiration process from a perforated shell;

– influences of the hole diameter and melt properties on the radial velocity field were determined and shown;

– optimal conditions for prilling in a rotating vibration granulator for a given capacity of 37 t/h are defined: the rotation velocity of the basket (60 rpm), the diameter of holes in the perforated shell (1.2 mm), the melt temperature (185 ^{o}C), the frequency range of the actuator's oscillation (340-400 Hz);

– the experimental studies and mathematical modeling provided possibilities for construction of a modernized rotating vibration granulator;

– industrial tests of the modernized vibrating granulator confirmed optimal conditions of the prilling resulting in the improved product.

1.2 Improving of the electronic intellectual cleaning system of holes in perforated shells of the priller

This report section is prepared in according to data [4].

The improvement of the prillers operation and quality of the obtained product has been achieved by creating the intellectual system to form the monodispersed drops in the dispersed devices, based on the electromagnetic vibrator [5]. This system enabled:

– to regulate the average size of the obtained granules, depending on the air temperature at the entrance to the granulation tower;

– to receive the stable size of granules, which does do not depend on the load (flow rate) of the fusion for priller;

– to reduce the heating load on the tower;

– to decrease the fraction content of granules of less than 1.0 mm in the product to 0.1-0.2% and dust in the air at the entrance of the tower by 20-60%.

At the same time, the market demands led to the necessity to produce goods with additives (for example porous ammonium nitrate, calcium-ammonium nitrate of the CAN trademark containing 25-28% of nitrogen). In the production of these fertilizers the powdered substances or liquid components, which contain particles larger than 0.4 mm, are fed into the nitrogen fertilizer fusion. These particles come to the holes of the perforated shell and cause full or partial clogging. It leads to:

– increase of the fusion level in the perforated shell of the priller;

– changes in the jet motion trajectory, that causes the sticking of the product to the workspaces in the tower;

– vibration system of the priller works in the non-optimal mode in case of the increased fusion level;

– deterioration of the granulometric composition of the product.

Table 3 –Description of the priller operation

Load on the priller by the fusion of the ammonium nitrate, t/hour	40	41	40
Level of the fusion in the perforated shell of the prillers, m	0.150	0.240	0.290
The fraction content is less than 1.0 mm in the product	0.1	0.4	1.1

As it is seen from the demonstrated data regarding the priller operation, the clogging of the holes in the perforated shell leads to the great increase of the fusion level in it and dust content rise in the product.

In order to remove the clogging of holes in the priller, the melt is stopped to flow and steam is fed or it is stopped to work, is demounted. The perforated shell and inner constructions of the priller are cleaned. During one day such cleaning can be carried out 3–15 times. It leads to the great losses of goods, unstable production.

In order to clean the holes in the perforated shell of the priller without stopping its work, it is reasonable to use high-frequency vibration. Such frequency can be periodically transmitted to the perforated shell of the priller.

Based on the above, the main aim of this research is to create the electronic intellectual system to regulate the formation of the monodispersed drops in the granulation devices and to clean their holes when they are clogged.

The high-frequency vibration is imposed on the perforated shell 6 by the high-frequency vibrator 9 (figure 1) in two modes:

– periodically in some time τ;

– when a certain level of the liquid is achieved in the perforated shell 6.

In the first mode of the holes cleaning in the perforated shell, the variable parameters included the duration of the high-frequency vibrator impulse, its amplitude, vibration frequency, the liquid level in the shell before and after the vibration overlay.

In the second mode of the holes cleaning in the perforated shell, the variable parameters included the amplitude of the high-frequency vibrator impulse and its vibration frequency. The operation o the high-frequency vibrator was based on the intellectual system and carried out to the value of the liquid level in the basket which was closer to the total cleaning of the holes.

The monodispersed fragmentation of drops was fixed as indicators of the device operation.

The level of liquid in the perforated shell

$$H = \frac{\left(\frac{4G}{n\pi d^2 \mu}\right)^2}{2g}, \qquad (26)$$

where G – flow rate of the liquid phase, m^3/hour; n – number of holes in the perforated shell; d – diameter of holes in the perforated shell, m; φ – jet compression coefficient; g – gravitational acceleration, m/s^2.

The structure and operating principle of the cleaning system of the holes in the perforated shell

The cleaning system of the holes in the perforated shell consists of the control panel and the high-frequency generator. The high-frequency generator is used to generate vibrations on the perforated shell of the priller.

Block-diagram of the high-frequency vibrator operation according to the second variant:

1. The income parameters: the liquid level in the perforated shell H, liquid flow rate G.

2. Determining of H.

3. Comparing

if Hi < H + xH →yes → to turn off the high-frequency vibrator;

→no → to switch on the high-frequency vibrator.

The main parameters and properties:

– Microprocessor – PIC16F877A:
– Frequency interval – 10Hz-10MHz;
– The frequency setting error of the high-frequency signal generator – 0.01.
– Frequency instability in 5 minutes of the work – $1 \cdot 10^{-5} f$.
– Signal output level – 2W.
– The output level setting error of the high-frequency signal generator – 10%.
– Harmonic components level – 30dB.
– Parasitic amplitude modulation – 0.3%.
– Parasitic numerical modulation of a high-frequency signal generator – $3 \cdot 10^{-6} f$.

Amplitude modulation mode:

– modulation coefficient – 0%-99%;

– error of the device / installation error – 10%;

– modulating frequency range – 0,05kHz-10kHz.

The cleaning system consists of the control panel and the high-frequency vibrator.

The control panel regulates the liquid level in the perforated shell of the priller, amplitude and frequency of vibration. The panel is implemented on the microprocessor. Thereby, it possesses high stability in the work and installation simplicity. The device lets to keep settings in the non-volatile memory, which can be easily changed depending on the exploitation conditions of the priller. The control panel has a built-in protection system against overload, overheating and a system of the "soft start".

To supply the whole device with power, the power source, made according to the classical scheme of the transformer, is used.

The installation of such a vibration system enables to:

– indirectly assess the degree of the holes clogging in the perforated shell of the priller;

– clean the holes in the perforated shell without stopping the priller and production as a whole;

– if it is necessary, the system lets to control the priller operation, using a PC;

– obtain the high-qualitative fractional composition of the final product;

– simplify technical service of the priller;

– use more reliable prilling system in the production.

All control elements are on the front panel. The printed boards of the device are treated with a protective varnish. The device has the built-in system, which lets to leave the "hangup" state if there are any failures in the program (as a rule, caused by the external factors – by welding, strong electromagnetic field, etc.).

The electric intellectual cleaning system scheme of perforated shell holes in the priller is demonstrated in figure 10.

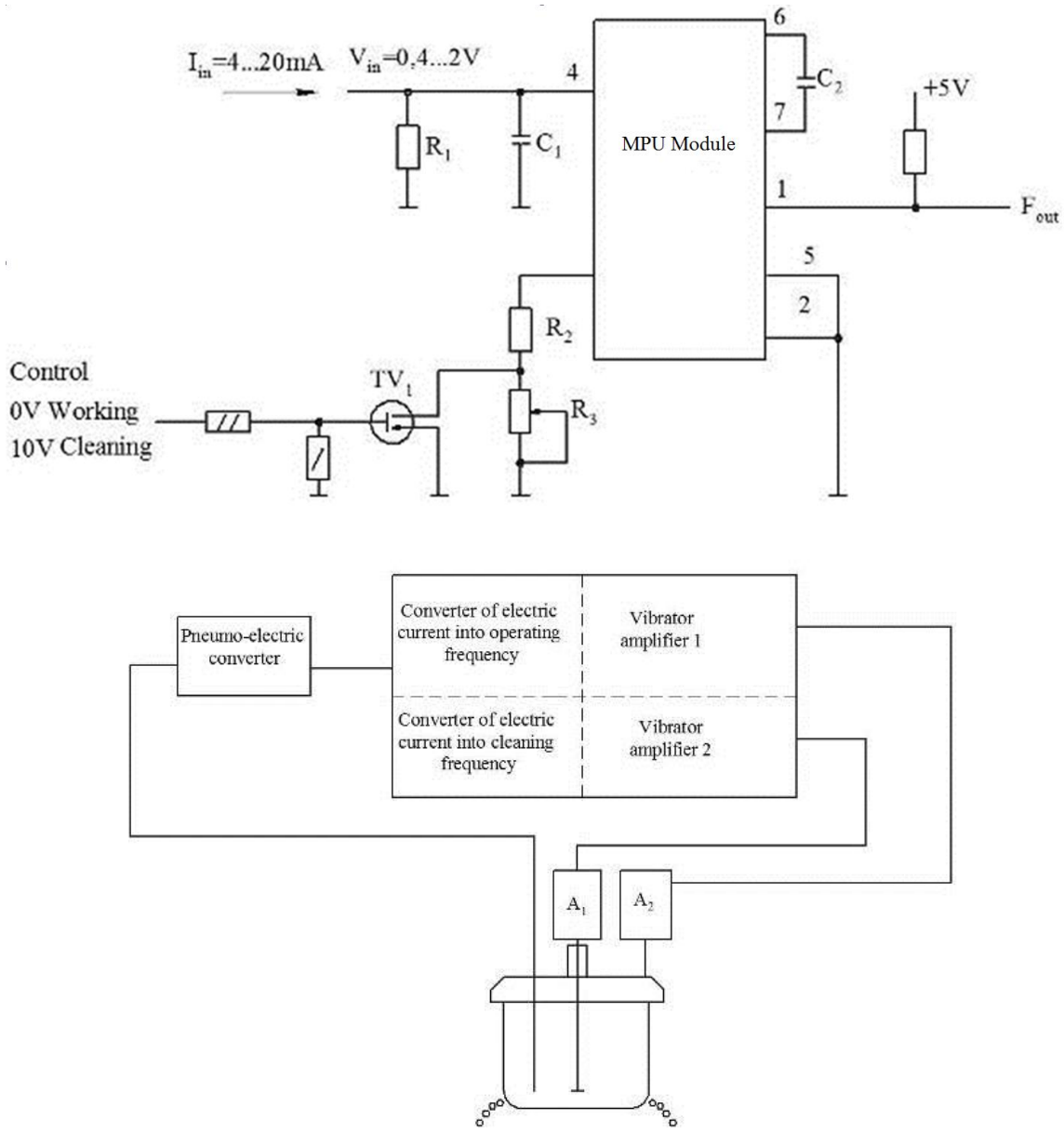

Figure 10 – The scheme of the vibrator operation

The scheme works in the following way.

The input current I_{in}=4…20mA is converted into the voltage V_{in}=0.4…2V on the resistor R_1. The input voltage U_{in} comes to the microcircuit DA_1 point 4 and is converted into the frequency according to the equations (2) and (3). If the control (control panel) is supplied with a voltage of about 0V, the frequency will be changed depending on I_{in} by the equation (2). If the control (control panel) is supplied with a voltage of 10 V, the transistor TV_1 will be opened and resistor R_3 will be shorted out and the equation (3) will be used in the predetermined range (cleaning mode).

$$F_{out} = \frac{U_{in}}{10(R_2 + R_3)C_2}, \tag{27}$$

$$F_{in} = \frac{U_{in}}{10R_2C_2}. \tag{28}$$

During the operation of the vibration priller owing to some additives the perforated basket is clogged in the fusion. It decreases the granulator productivity, worsens the fusion jet properties and increases dust formation. One of the most significant constituents of the nitrogen-containing fertilizers losses at the production stage is dust emission from fertilizers with cooling air into the atmosphere. For example, ammonium nitrate production unit AN - 60, with a gas flow rate of 300 thousand m^3/hour through the tower and containing the ammonium nitrate dust of 200-250 mg/m^3, annually emits over 1500 tons of the nitrogen fertilizer into the air. Therefore, the ammonium nitrate dust amount, which is in the air of the tower, can reach 0.8 g/m^3. It causes the product losses and requires additional cost for the purification of the air coming out of the tower. Together with an economic aspect, related to the energy- and resource cost, this problem has also an ecological one – pollution of the air basin, transfer of fertilizers into the surface and groundwater, accumulation of nitrites and nitrates in the plants and waters, that leads to the load on the ecosystem. The results of the experimental and industrial testings of the modified prillers with the proposed intellectual system in the ammonium nitrate production demonstrated the efficiency of the changes, introduced into the system, and enabled to reduce the economic and ecological damage in the production of the nitrogen mineral fertilizers. Using the control panel of the vibration frequency, the system lets to impose high-frequency oscillations on the perforated shell of the priller, which cause to the cleaning of holes from pollutions. The proposed electric intellectual system has been tested and ways of its further improvement have been outlined. Implementation of the improving electronic intellectual cleaning system of holes allowed reducing the error in the high-frequency oscillations on the perforated shell of the priller from 0,43 to 0,27, i.e. 1,6 times.

2 RESEARCH OF THE PROCESS OF THE GRANULATION AND DRYING OF MINERAL FERTILIZERS IN THE DEVICES WITH ACTIVE HYDRODYNAMICS

2.1 Operational regimes in the devices with active hydrodynamics

This report section is prepared in according to data [5-8].

Ansys CFX and Ansys Fluent (https://www.ansys.com) software is based on a finite-volume method of solving hydrodynamic equations and using a rectangular adaptive mesh with local grinding. In order to approximate curvilinear geometry with higher accuracy, the technology of geometry grid density is used. This technology enables to import geometry from CAD systems and to share information with finite element analysis systems. This technology has solved the problem of automatic mesh generation – in order to generate a mesh, it is enough to set only a few parameters, after which the mesh is automatically generated for a computational area that has the geometry of any complexity degree.

The calculation starts with some initial approximation set as the initial data. At each global iteration, the velocity and pressure fields, obtained after the time specified as the integration step, are calculated. The stationary solution of the problem is achieved after a sufficiently large number of global iterations corresponding to a long period of time.

When performing the calculation, the program automatically breaks the calculation area into separate subareas, subdomains, the size of which is proportional to the velocity of the appropriate processor. The calculation algorithm works in such a way that each processor calculates the flow only in its own subdomain, and after each global iteration, the resulting solution is “adhesion”. The parallelization algorithms used in modern software products let to achieve acceleration with an efficiency close to 100%. In other words, the calculation time is inversely proportional to the total computing power

As a rule, the adhesion condition is set as boundary conditions on all solid walls (the velocity is zero), the distribution of all velocity components in the inlet section, and

the first derivatives (in the direction of flow) of the velocity components in the outlet section are equal to zero. In practice, if the flow rate at the inlet is approximately uniform in the intersection, the user sets only the average velocity (or flow rate) at the inlet, and sets nothing at the output - it is assumed that the user chose the output section far enough from the areas of intensive restructuring of the flow.

Vortex granulator

Regime I. Gas flow filtering through the stationary layer of granules (figure 11a). The layer is motionless, gas flow passes through pores in the layer.

Regime II. Beginning of the granules layer motion (figure 11b). In this regime, the lower parts of the layer are partially weighted, while the upper parts of the layer are still motionless.

Regime III. Partially fluidized bed (figure 11c). Granules in the lower parts of the layer are in the weighted state and move along the circular trajectory with low intensity, the granules in the upper parts of the layer are motionless. At a certain gas velocity, the whole layer goes into the weighted state.

Regime IV. Fluidized bed with partial swirling (figure 11d). Granules in the weighted layer take the wave trajectory, which is characterized by the localized vortex motion, started in any random place of the layer. The vortex is spread in that part of the layer, which is above the gap of the gas-distributing device, and the rest of the area is in the suspended state. With an increase of the gas velocity, the growing number of granules is drawn into the vortex motion.

Regime V. Developed vortex fluidized bed (figure 11e). With further increase of the gas velocity, the process of waves formation is weakened, the weighted layer has the ordered vortex structure.

Regime VI. Stable ablation regime of granules (figure 11f). Space over the vortex weighted layer of the material is filled with the solid phase, and the difference between the vortex weighted layer and overlayer space consists only in the concentration of the solid material. There is a gradual reduction of the granules concentration in the overlayer space with an increase of the height. Granules leave the vortex layer; their

ablation is caused by the domination of the upward flow gas force over the gravity force.

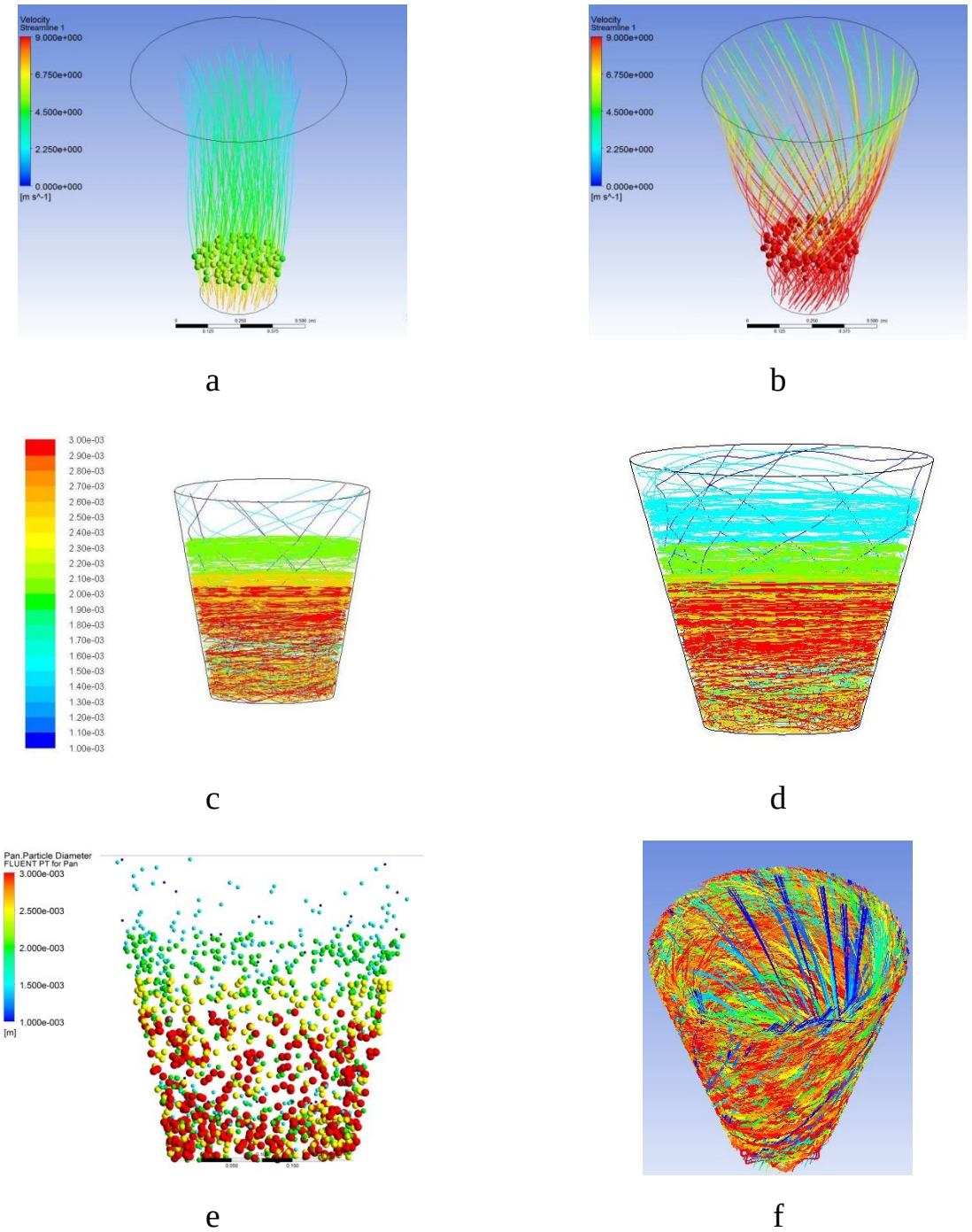

Figure 11 – Typical regimes of the vortex granulator operation: a – gas flow filtering through stationary layer of granules; b – beginning of the granules layer motion; c – partially fluidized bed; d – fluidized bed with partial swirling; e – developed vortex fluidized bed; f –stable ablation regime of granules

Shelf multistage device with a weighted layer.

In the upper section of the device the inclined shelves (angle of lean 30°) with ratio l/B (where l is the distance from the end of the shelf to the wall of the device; B – width of the device) in the amount of l/B=1 (free channel) to l/B=0.3 were installed. The results of the previous investigations, show that the efficiency to extract the small fraction (with the size less than 1 mm) into the ablation has the maximum value with the ratio l/B=0.5.

Thus, at the first stage of theoretical studies, it was necessary to find the optimal value of the free area in the shelf for the ablation efficiency of the fraction less than 1mm.

The results of the computer modeling show that the efficiency to extract the small fraction into the ablation is achieved with the reduction of the perforation degree of the shelf. While installing the solid shelf in the separation zone of the device, the whole gas flow guaranteedly passes through the outloading space. It defines the extraction of the small fraction of the material precisely in this zone. 5 % of perforation in the shelf causes the redistribution of the gas flow, directing its share through the hole in the shelf. Therefore, the gas flow intensively is interconnected with the material and not only in the outloading space zone but also on the shelf surface. It causes the increase of the fraction ablation efficiency, which is less than 1 mm.

The further increase of the free area of the inclined contact shelf is followed by the reduction of the small fraction extraction efficiency into the ablation. It is explained by the increased effect of the gas flow redistribution. The gas flow velocity in the outloading space decreases so much that the small fraction extraction process of the material in this zone is not very intensive. The total area of holes does not provide sufficient phase contact.

There are three perforated shelves in the drying (granulation) zone of the device. Moreover, while changing the distance between the end of the shelf and the wall of the device, it is possible to create different velocities of the gas flow

Regime I. Transition regime (figures 12a, 12b). The upward gas flow force in this regime causes the gradual change of its motion trajectory from the translational to the pulse-forward ones in direction of the outloading gap. Therefore the dispersed material starts to move into the weighted state, and the inertial force is compensated by the upward flow force of the drying agent.

Regime II. The weighted layer regime (figure 12c). The effect, made by the upward flow of the heat transfer agent in such regime leads to the creation of the stable weighted layer thanks to the compensation of the inertial force and the rolling-down force on the sloping surface. The gas flow velocity reaches the first critical value, then it increases and is within the range of the working velocity.

Regime III. The regime of the developed weighted layer (figure 12d). This regime is described by a dominant effect of the upward gas flow force on the dispersed material and by the increase of its displacement vertical component. Therefore, at first, the share of the dispersed material is taken out from the surface of the shelf and then it moves to the outloading gap.

In general, the algorithm to calculate the device with the directed fluidized bed can be represented by means of blocks (figure 13), which are logically interconnected between each other. The peculiarity of the algorithm includes its universality and ability of “flexible” implementation of separate blocks.

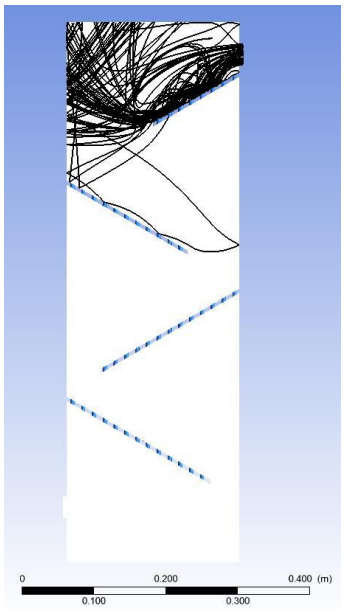

a

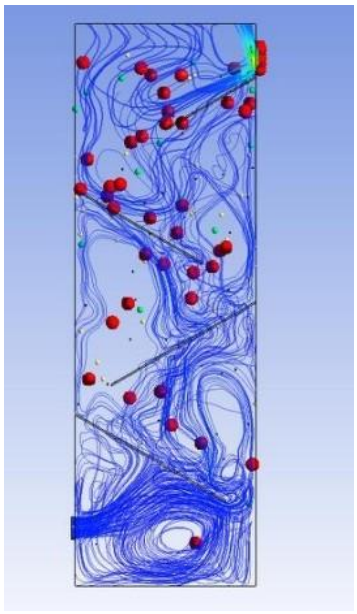

b

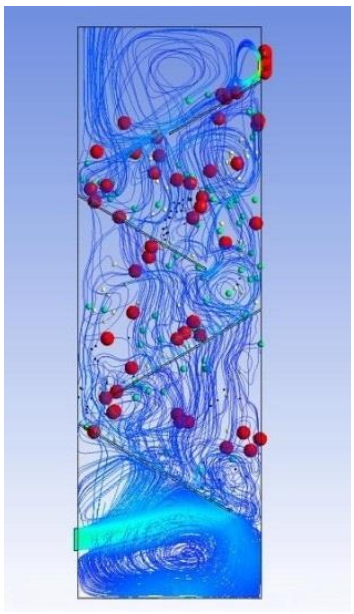

c

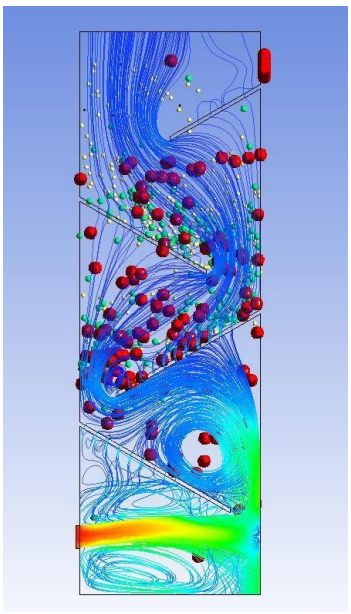

d

Figure 12 – Typical operation regimes of the shelf multistage device (dryer or granulator): a – separation of the small fraction in the shelf dryer (granulator); b – transition operation regime of the dryer (granulator); c –weighted layer regime of the dispersed material motion; d – developed weighted layer regime of the dispersed material motion

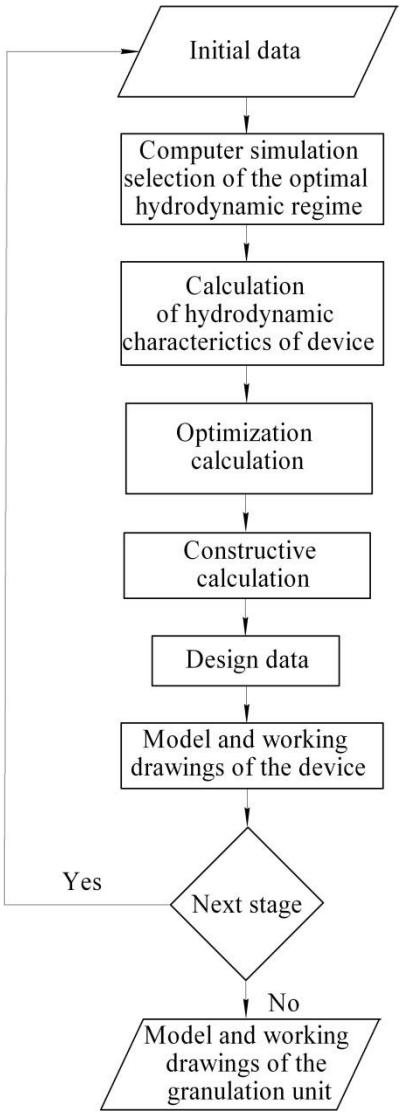

Figure 13 – Block-scheme of the granulation unit calculation

The modeling and calculation results with the use of authors' software, description of which is represented in the work [9], are exported to the cluster Granulation Unit© in the form of separate structural blocks (figure 14).

Figure 14 – Cluster Granulation Unit©

2.2 Convective drying in the multistage shelf dryers: theoretical bases

This report section is prepared in according to data [10-13].

The necessity to determine these features is due to the fact that before constructing an industrial sample of the gravitational shelf dryer it is necessary to determine its optimal design. In this case, the optimization criterion is to ensure the minimum required residence time of the dispersed phase in the working space of the dryer, which will let to complete the drying process to a predetermined humidity indicator. It is important to observe the condition, under which the “hydrodynamic” residence time of the dispersed phase in the workspace of the device should be no less than the “thermodynamic” time (this parameter is determined by the kinetics of the moisture removal process from the dispersed phase). Therefore, in order to keep the integrity of the dispersed particles, the "hydrodynamic" time should not exceed the "thermodynamic" time by more than 5-10%. By adjusting the hydrodynamic properties

of the flow, an optimal construction of the gravitational shelf dryer is achieved, which meets the requirements of the optimization criterion.

Thus, the optimization calculation of the dryer consists of three blocks: hydrodynamic calculation (calculation of the residence time of a particle on a stage), kinetic calculation (kinetic parameter of the moisture removal) and calculation of drying efficiency.

Initial data (figure 15):

– rate of gas flow Q, m^3/s;
– length of device L, m;
– overall width of device h, m;
– length of shelf L_s, m;
– degree of perforation (free area) δ;
– perforation hole diameter d, m;
– the tilt angle of shelf γ, degr;
– the radius of the granule r_{gr}, m;
– granule density ρ_{gr}, kg/m^3;
– gas density ρ_g, kg/m^3;
– acceleration of gravity g, m/s^2;
– resistance coefficient ξ;
– volumetric content of a dispersed phase in a two-phase flow ψ;
– the coefficient that takes into account the tightness of the flow m;
– number of stages in dryer i.
– moisture of the material i-stage of the dryer x, kg of water/kg of material;
– moisture of the drying agent in i-stage of the dryer b, kg of water/kg of material;

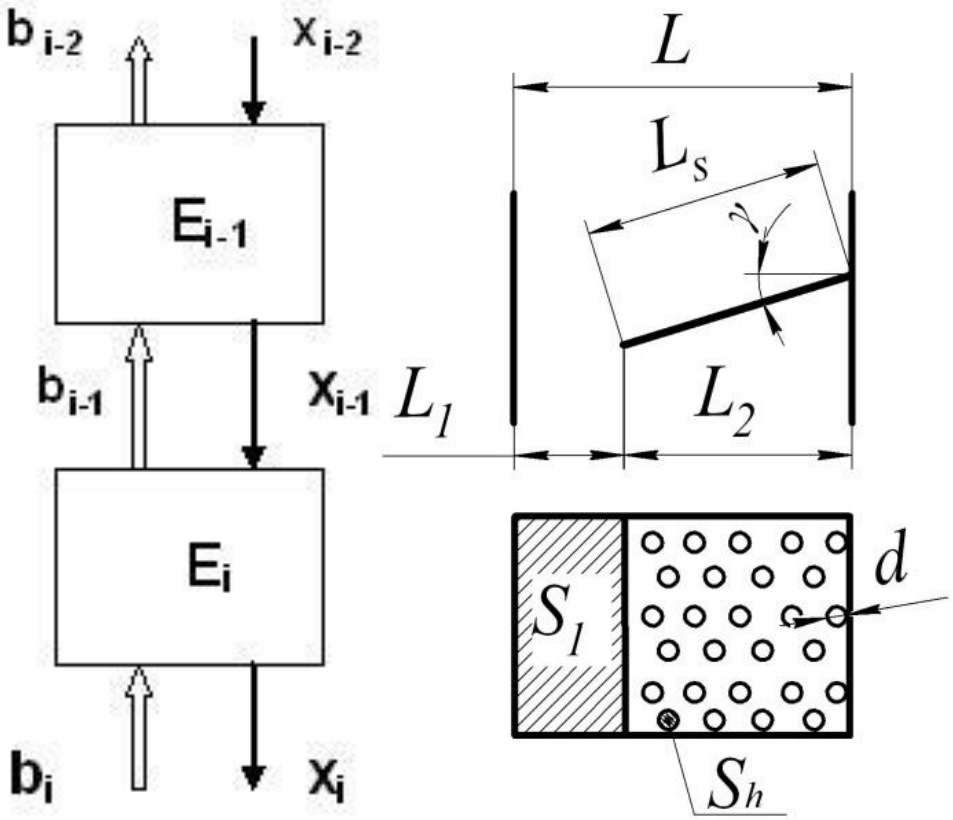

Figure 15 – A fragment of the calculation scheme for the multistage drying: left figure – change of flows' moisture; x– moisture of the disperse material; b – moisture of the drying agent), right figure – construction of dryer's workspace

Hydrodynamic calculation

Hole area on the shelf (horizontal position), m^2

$$S_h = \frac{\pi d^2}{4}. \tag{29}$$

The perforated area on the shelf (horizontal position of the shelf), m^2

$$\sum S_h = L_s \cdot h \cdot \delta. \tag{30}$$

Number of holes on the shelf

$$n = \frac{\sum S_h}{S_h}. \tag{31}$$

Area of outloading clearance, m^2

$$S_1 = (L - L_s \cos\gamma) \cdot h. \tag{32}$$

Area of the gas passage holes in the shelf (inclined position of the shelf), m^2

$$S_2 = \frac{\pi d^2}{4} \cdot n \cdot \cos\gamma. \tag{33}$$

The relative area of outloading clearance

$$S_1^r = \frac{S_1}{S_1 + S_2}. \tag{34}$$

The relative area of the gas passage holes in the shelf

$$S_2^r = \frac{S_2}{S_1 + S_2}. \tag{35}$$

Rate of the gas flow in outloading clearance, m^3/s

$$Q_1 = Q \cdot S_1^r. \tag{36}$$

Rate of the gas flow in holes in the shelf, m^3/s

$$Q_2 = Q \cdot S_2^r. \tag{37}$$

Gas velocity in holes in the shelf, m/s

$$V_{work} = Q_2 / S_2 . \quad (38)$$

Second critical velocity, m/s

$$V_{cr} = 1,63 \cdot \sqrt{\frac{\rho_{dr} \cdot g \cdot r_{gr}}{\xi \cdot \rho_g}}. \quad (39)$$

Velocity difference, m/s

$$\Delta V = V_{cr} - V_{work}. \quad (40)$$

Time of material residence on the shelf (free movement), s

$$\tau_f = \frac{L_s}{\Delta V \sin \gamma}. \quad (41)$$

The empirical function of the effect of compression on the residence time of the particle in the working space of the device

$$f_{e\tau}(\psi) = (1-\psi)^{-m}. \quad (42)$$

Time of material residence on the shelf (straitened movement), s

$$\tau_s = \frac{L_s \cdot f_{e\tau}(\psi)}{\Delta V \sin \gamma}. \quad (43)$$

The program Multistage fluidizer® used Hyper markup language HTML, cascading style sheet (CSS) and programing language JavaScript (including the library JQuery). HTML is presented as a tagging of web-based app, CSS pages formatting. JavaScript is used to calculate and to transfer data, to create animation and data validation effect. In the validation block of JavaScript, data accuracy is checked. In the block input info, basic data fields indices are accepted and they are written to the object of input_information. In the block, calculation computations are carried out by equations (29)-(43).

Index.html (figure 16) is the main page of the web-based app. It is responsible for reflection of the main menu, for main calculation of gas flow and for jumping the other pages (an examples of such page is represented in the figure 17), where main dependencies between key features to calculate gas flow and resistance time of the material on the shelf, are calculated and dependencies diagrams are formed.

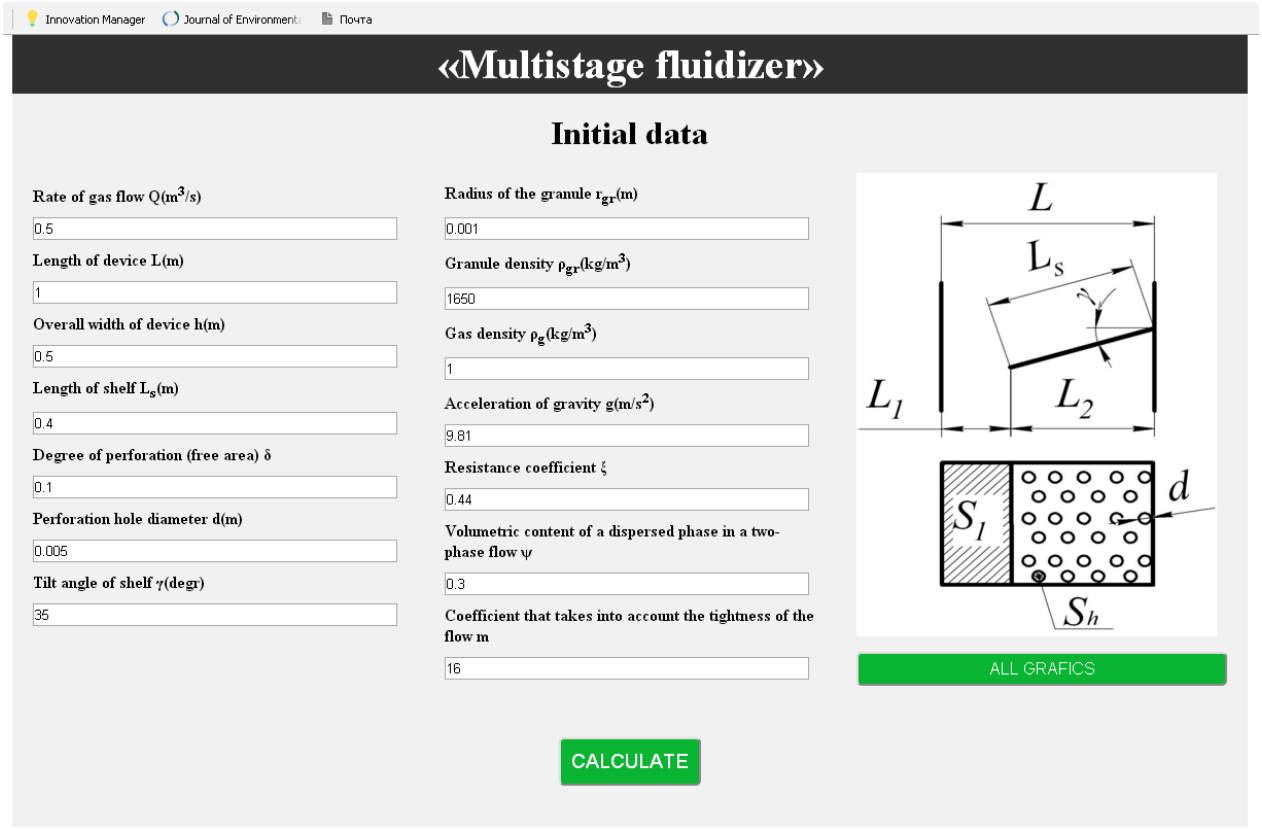

Figure16 – The main page of the Multistage fluidizer® software

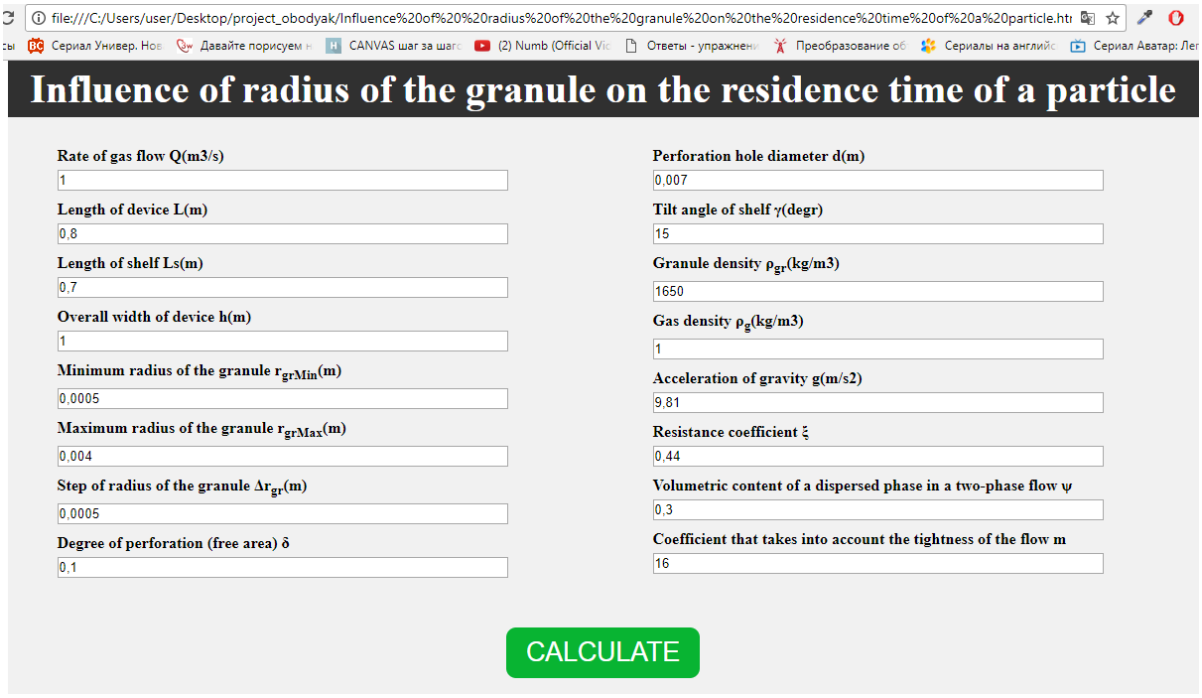

Figure 17 – Calculation page of various parameters impact on the particles resistance time in the device

Having inserted data, data validity is tested, if all data is correct, after keystroke CALCULATE data is processed given the above formulas and we receive the result in form of the computation table (figure 18).

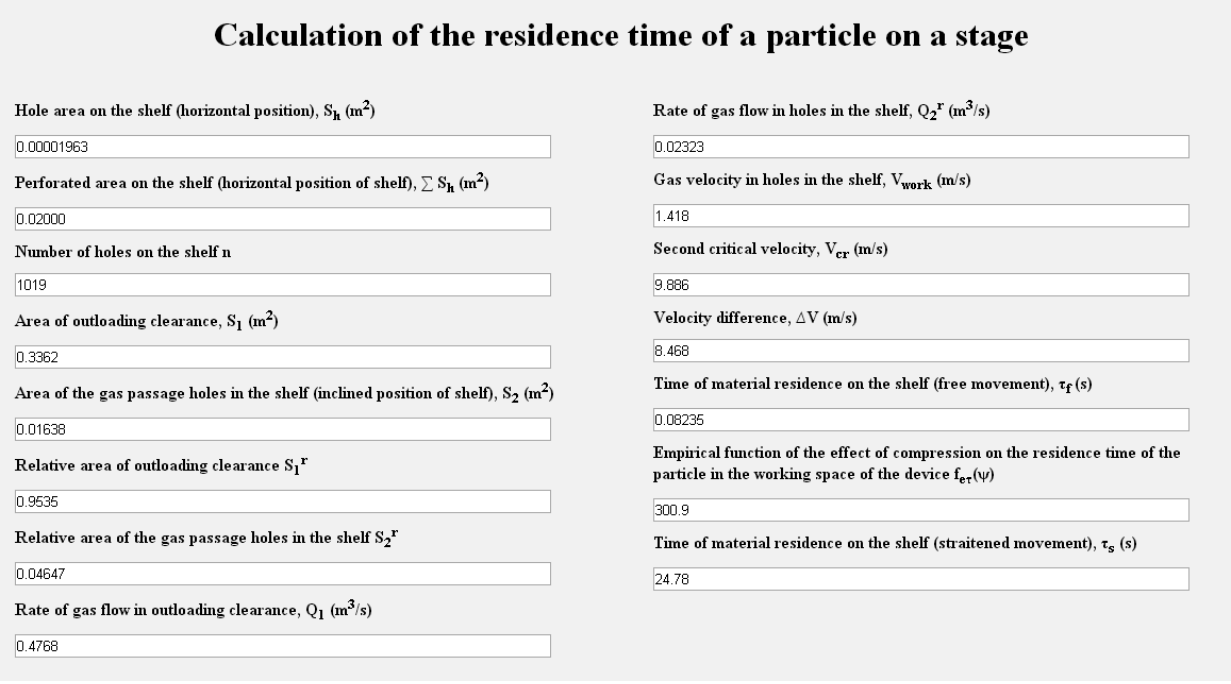

Figure 18 – Results of calculation

After changes of indices l_f and l_s it is possible to see how the animation appears while pressing the button show calculation (the example of distance length calculation, which particle takes on the shelf during the specified period of time, is shown in the figure 19). In order to create animation, functions clicker_lf and clicker_ls are implemented respectively for τ_f and τ_s animation.

In JavaScript one uses: libraries JQuery and table2excel, objects for data recording, methods .val(), .append() to read and to insert indices to fields, methods .removeClass() and .addClass() to delete and to add classes, method .animate() for work with animation lets to create an animation effect for any digital CSS feature of the element.

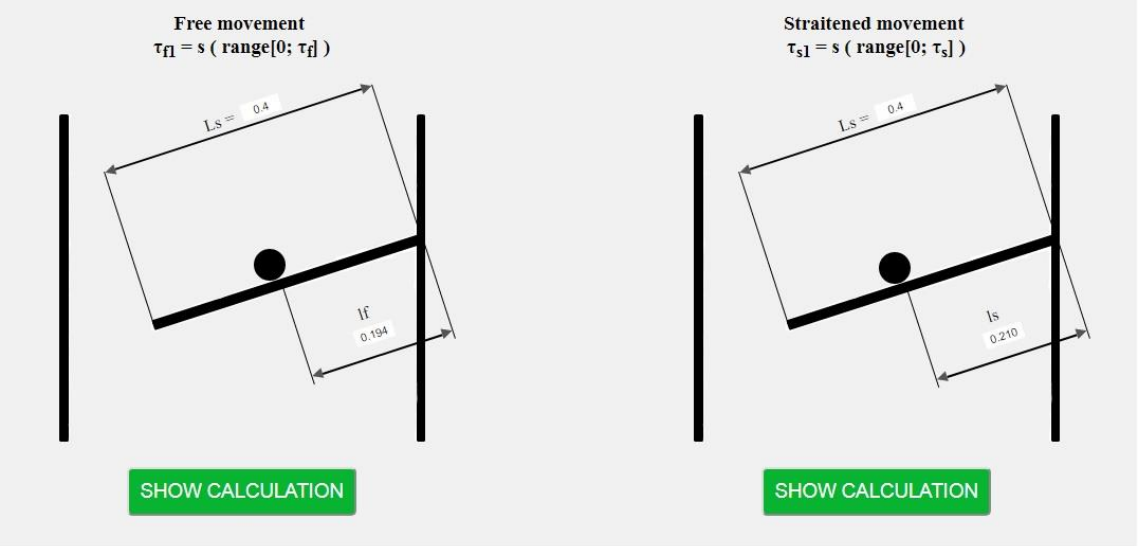

Figure 19 – Calculation of way length, which particle undergoes on the shelf during the specified period of time

In order to calculate the kinetic parameter of the moisture removal (the moisture-yielding capacity coefficient) let us use the following algorithm.

It is proposed to use the following equation for calculation of β:

$$\frac{\Delta U_m}{\tau} = \beta \cdot F \cdot \left(b_{fin} - \frac{b_{fin} + b_{in}}{2} \right) \cdot \rho_g, \tag{44}$$

where b_{in}, b_{fin}, ΔU_m – the initial and final humidity of the drying agent, amount of the removed moisture from the material; F – the surface of the mass transfer, which depends on the dryer's effective operation due to the disperse material and the residence time of the material in the dryer.

In general, the criteria equation of the drying process can be written as follows:

$$Sh = A_1 \cdot Sc^n \cdot \mathrm{Re}^m, \tag{45}$$

where A_1 – the equation coefficient; $Sh = \beta \cdot d_{gre} / D$ – Sherwood criterion; d_{gre} – equivalent diameter of the particle (granule), m; $Sc = \nu / D$ – Schmidt criterion; $\mathrm{Re} = \left(V_{work} \cdot d_{gre}\right) / \nu$ – Reynolds criterion; D – diffusion coefficient of the gas flow, m^2/s; ν – kinematic viscosity coefficient of the gas flow, m^2/s; m, n – indicators of the equation stages, which are evaluated through the graphical dependency $Sh / Sc^{0,33} = f(Re)$, obtained from the experimental data.

The drying process effectiveness on the i-stage of the dryer is presented by the ratio of differences between the moisture contents of the disperse material before and after the drying x_{i-1}-x_i to the maximum possible (theoretical) difference between the moisture contents on the stage $x_{i-1} - b_i$, and also in the form of the function of the kinetic parameter of the moisture transfer B_i, the residence time of the material on the stage τ_i and the consumption ratio of the dispersed phase to the drying agent G_i^{-1}

$$E_i = \frac{\Delta x}{\Delta x_{\max}} = \frac{x_{i-1} - x_i}{x_{i-1} - b_i} = \frac{1 - \exp\left[-\beta_i \tau_i (1 + G_i^{-1})\right]}{1 + G_i^{-1}}. \tag{46}$$

Some graphic dependencies are shown in the figure 20. The program lets to receive two- and three-dimensional dependency graphs.

In general dependencies diagrams, features for free and constraint motion of particles have one functional dependence. The particle resistance time has enough narrow diapason at every stage (shelf) in free motion regime and is calculated by seconds units. In the constraint motion regime of particles, the residence time is greatly increased at every stage. The abundant ratio of particles in the two-phase system has a definite impact on this index. That is why, while defining the optimum performance of the device, it is necessary to define the workspace size of the granulating or drying device to high accuracy.

The impact made by some constructive features of the shelf dryer during the residence time of the dispersed material (figure 20) is shown below.

The change of the shelf tilt angle to the horizon affects the redistribution of the gravity components: enlargement of it leads to an increase of the gravity rolling component and vice versa. It should be mentioned that the tilt angle of the shelf may have a minimum value that complies with the natural slope angle of the material. As the tilt angle of the shelf decreases, the residence time of the dispersed material gradually increases. It leads to longer contact with the drying agent's flow.

Changing the gap between the edge of the shelf and the dryer's wall significantly influences the change of the residence time of the dispersed material on the shelf. If the gap increases, the contact time of the dispersed material with the drying agent will be reduced due to the decrease in the length of the material movement distance on the shelf. In this case, the operation of the rolling component of the dispersed material velocity lasts for a shorter period and at the end of the shelf is replaced by the full gravity. Thus, the material moves down and only the ascending gas flow force resists its fall.

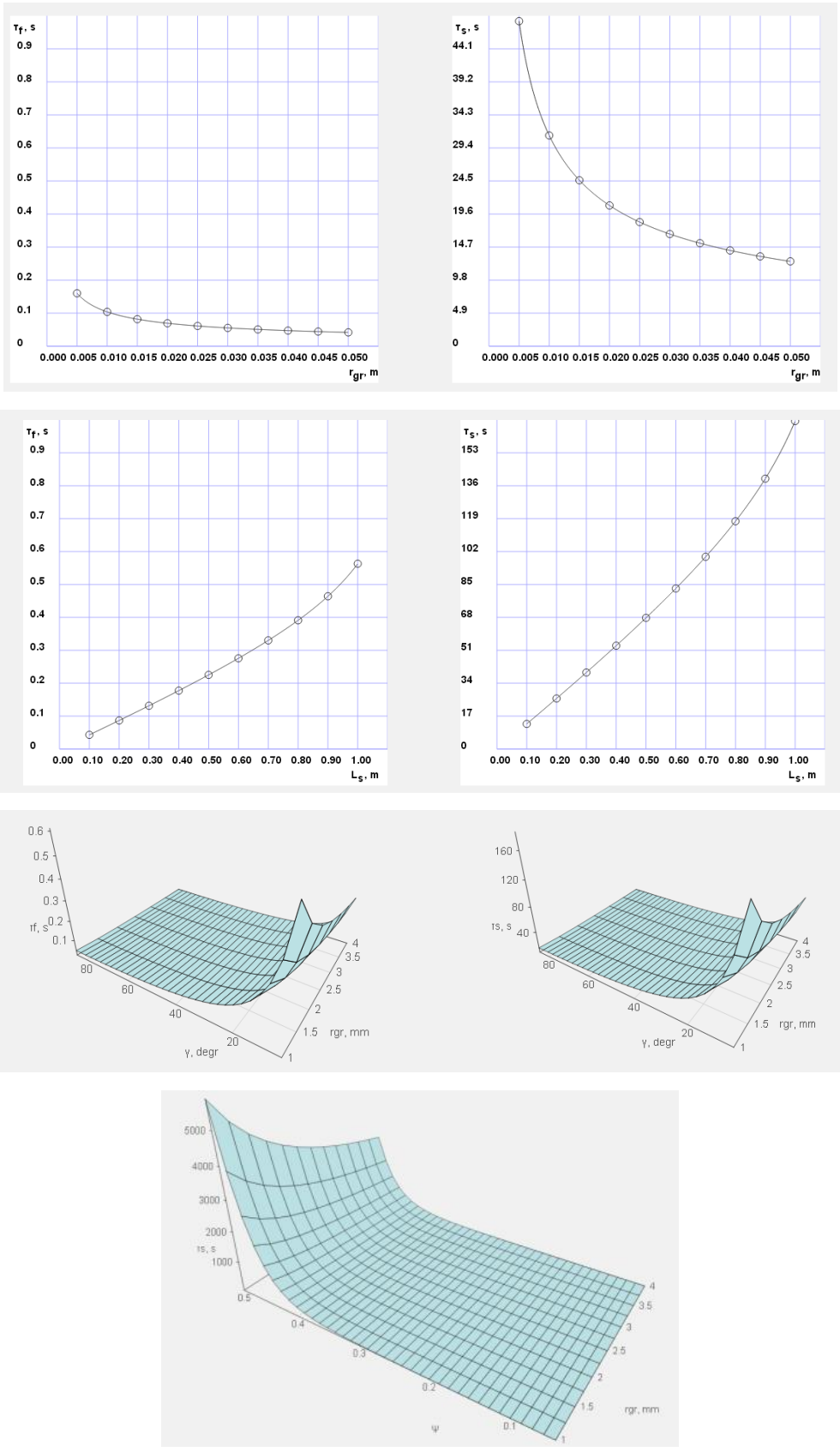

Figure 20 – Examples of calculation results

The analysis of the calculations regarding the effect, made by the free cross-sectional area of the shelf on the drying process efficiency showed the following. Reducing the free cross-sectional area of the shelf leads to an increase of the drying agent's ascending motion velocity in the holes. In this case, the action of the drying agent's ascending flow slows down the progressive motion of the dispersed material on the shelf, compensating for the rolling component of its gravity. The pulse component of the dispersed material displacement decreases and the trajectory changes to a pulse-forward one. The trajectory length of the dispersed material motion increases, the time of its contact with the drying agent is extended.

As the diameter of the perforation holes decreases, the effect of the drying agent's ascending flow increases, in which the pulse component of the dispersed material motion trajectory decreases, and the forward - increases. Thus, the trajectory length of the dispersed material motion increases and the contact time with the drying agent is extended. It should be noted that with the further reduction of the perforation holes diameter, the action of the drying agent's ascending flow begins significantly to outweigh the effect of the gravity rolling component. It leads to the formation of the second transitional mode and the ablation mode in the shelf dryer's operation.

The calculated values of the mass transfer coefficient β from the equation (44) depending on the velocity of the drying agent's motion, is demonstrated in figure 21.

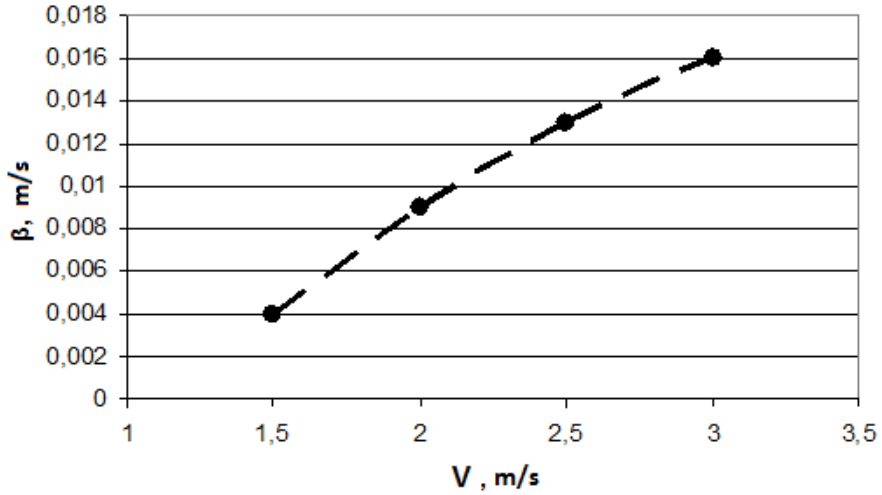

Figure 21 – Dependence of the mass transfer coefficient on the drying agent's motion velocity

The graphical dependency from the equation (45) shows (figure 22) that coefficient A_1= 0,008, m = 0,47. The coefficient n is 0.33 for the situation when the drying agent's parameters were slightly changed during the experiment.

Taking into account the obtained values of the coefficient A_1 and equation stage m, the criterial value (46) will be as follows:

$$Sh = 0,008 \cdot Sc^{0,33} \cdot \mathrm{Re}^{0,47} \tag{47}$$

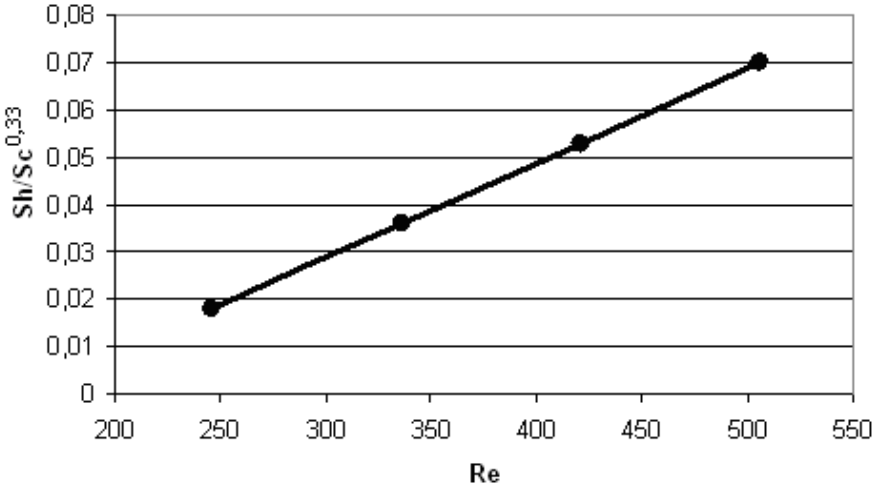

Figure 22 – Graphical dependency $Sh / Sc^{0,33} = f(Re)$ to define the coefficient A_1 and equation stage m.

The organization of the drying agent's motion may have a considerable influence on the quality indicators of the dried material and the properties of the drying agent. That has evolved several studies, the results of which are presented in figures 23-26. Their analysis enables us to select the method to organize the drying agent's motion, which consumes the least energy and ensures the necessary complete removal of moisture from the disperse material.

The analysis of the figures shows that the features of the dispersed material and the drying agent are changed according to one law; each of the technological indicators in the drying agent differently influences the intensity of the increase or decrease of parameters. The figures show that there is no function extremum on the graphical dependencies, which is explained by the regularities of the convective drying kinetics -

the parameters change of the contacting flows in each of the periods occurs monotonically with different intensity on separate sites depending on the dehydration conditions.

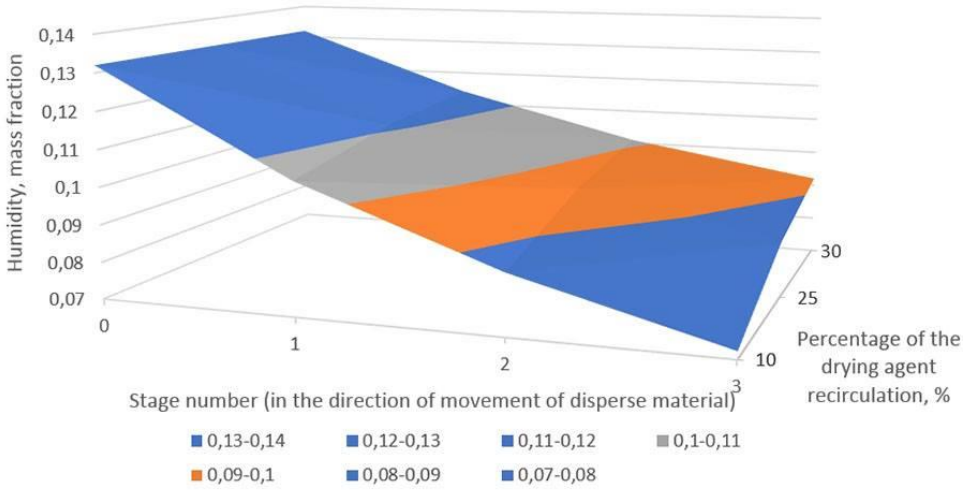

Figure 23 – Influence of the drying agent recirculation method on the change of the moisture content in the disperse material

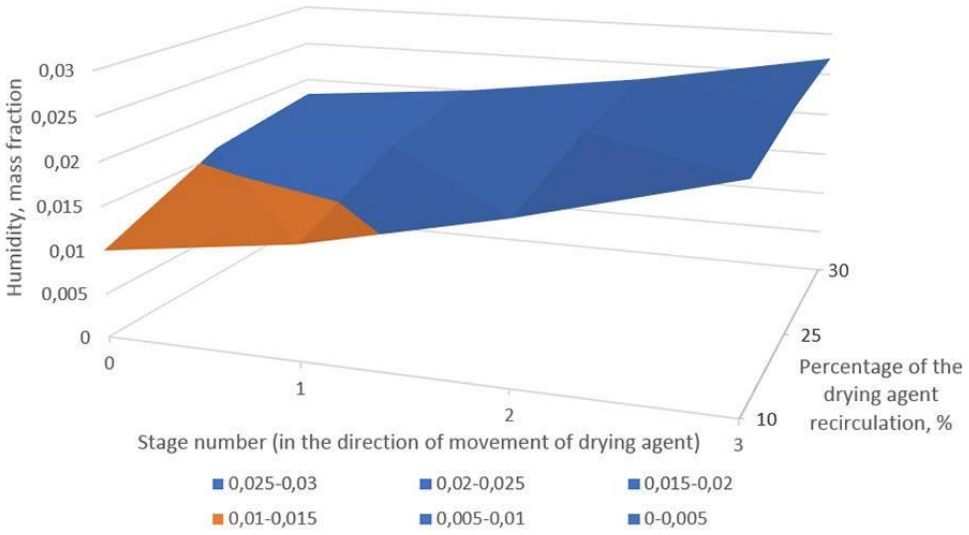

Figure 24 – Influence of the drying agent recirculation method on the change of the moisture content in the drying agent

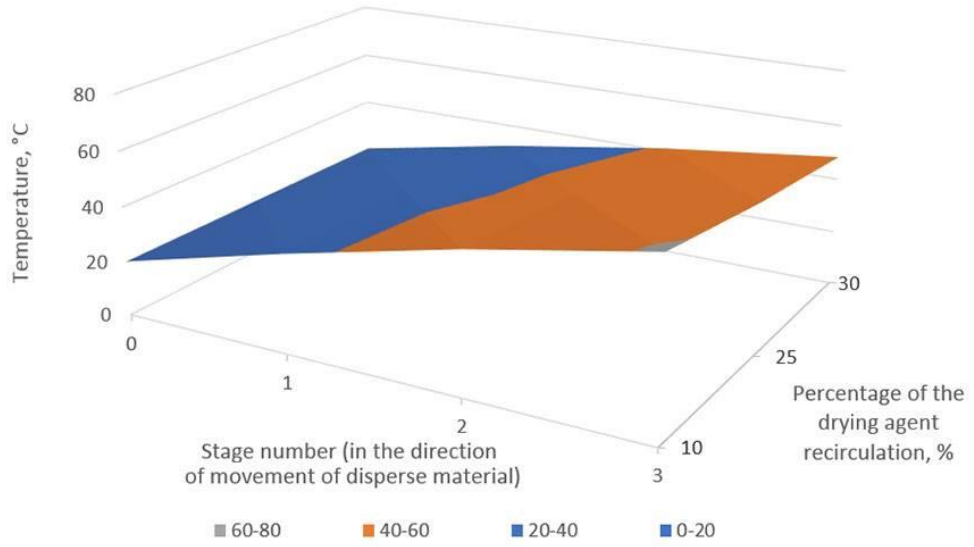

Figure 25 – Influence of the drying agent recirculation method on the temperature change of the disperse material

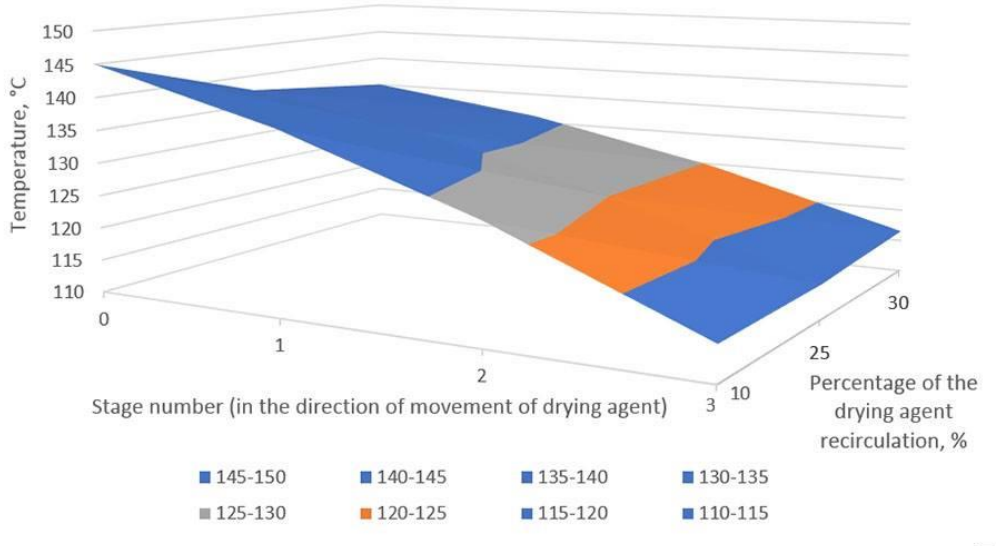

Figure 26 – An influence of the drying agent recirculation method on the temperature change of the drying agent

Block-scheme of the algorithm to calculate the multistage gravitational shelf dryer is represented in figure 27.

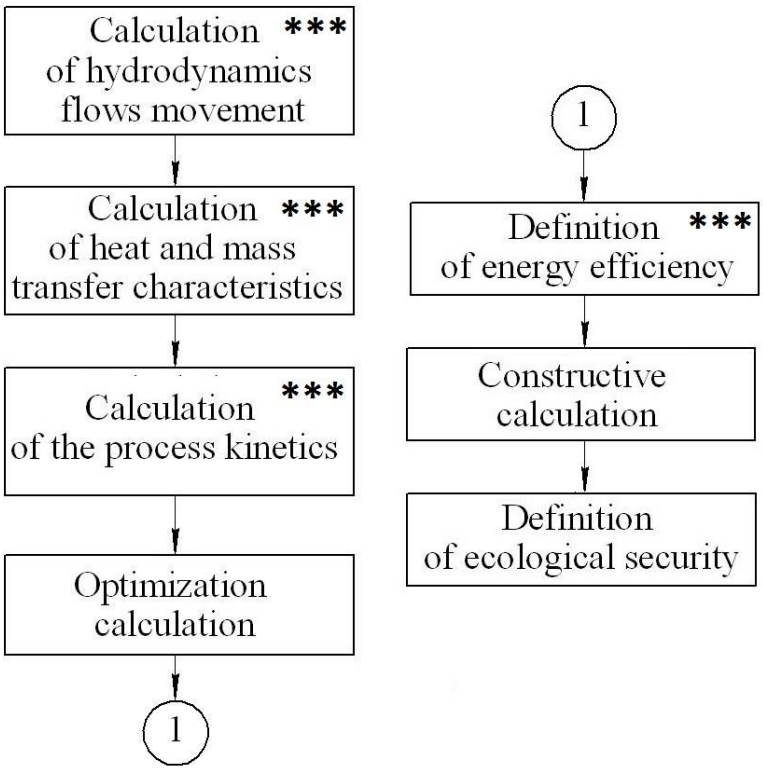

Figure 27 – Block-scheme of the algorithm to calculate the multistage gravitational shelf dryer (symbol *** shows the blocks which are described in this work).

CONCLUSIONS

- a mathematical model was derived to calculate hydrodynamic properties of the melt jet expiration process from a perforated shell;

- influences of the hole diameter and melt properties on the radial velocity field were determined and shown;

- optimal conditions for prilling in a rotating vibration granulator for a given capacity of 37 t/h are defined: the rotation velocity of the basket (60 rpm), the diameter of holes in the perforated shell (1.2 mm), the melt temperature (185 ^{o}C), the frequency range of the actuator's oscillation (340-400 Hz);

- the experimental studies and mathematical modeling provided possibilities for construction of a modernized rotating vibration granulator;

- industrial tests of the modernized vibrating granulator confirmed optimal conditions of the prilling resulting in the improved product.

- the proposed electric intellectual system has been tested and ways of its further improvement have been outlined. Implementation of the improving electronic intellectual cleaning system of holes allowed reducing the error in the high-frequency oscillations on the perforated shell of the priller from 0,43 to 0,27, i.e. 1,6 times;

- various hydrodynamic regimes to weigh particles of a material by a gas flow, depending on the constructive parameters of shelf contacts was showed;

- the effectiveness of the shelf device to carry out the drying and dedusting processes of granular and powder materials simultaneously was experimentally proved.

REFERENCES

1. Sklabinskyi V.I., Artyukhov A.E., Kononenko N.P., Krmela J. Decay of melt stream of during dispersion in granulation devices / Hemijska industrija. – 2019. - 73(4). – pp. 239-248.

2. Kreber [E-text type]. Location of document: https://www.kreber.nl/markets/prilling-nitrates date of access 22.12.2019.

3. Research Institute at the Chemical plant [E-text type]. Location of document: https://www.niichimmash.ru/ date of access 22.12.2019.

4. Sklabinskiy V., Skydanenko M., Kononenko M., Artyukhov A. Improving of the Electronic Intellectual Cleaning System of Holes in Perforated Shells of the Priller / Proceedings of the International Conference on Modern Electrical and Energy Systems, MEES 2019. – 2019. - pp. 70-73.

5. Artyukhov A., Sklabinskiy V., Ivaniia A. Electrical intelligent system for controlling the formation of monodisperse droplets in granulation devices based on magnetostrictive actuator / Proceedings of the International Conference on Modern Electrical and Energy Systems, MEES 2017, – 2017. - pp. 280-283.

6. Artyukhov A., Artyukhova N., Krmela J. Computer Simulation of the Aerodisperse Systems Hydrodynamics in Granulation and Drying Apparatus In: Process Analysis / Design and Intensification in Microfluidics and Chemical Engineering. – IGI Global, USA. – 2019. – pp. 277-321.

7. Obodiak V., Artyukhova N., Artyukhov A. Calculation of the residence time of dispersed phase in sectioned devices: Theoretical basics and software implementation / Lecture Notes in Mechanical Engineering. – 2020. - pp. 813-820.

8. Artyukhov A.E., Krmela J., Gavrylenko O.M. Evaluation of the Impact Made by the Hydrodynamic Regime of the Granulation Equipment Operation on the Nanoporous Structure of N_4HNO_3 Granules / J. Nano- Electron. Phys. – 2019. – 11 No 3, 03033-1-03033-4.

9. Рішення про реєстрацію договору, який стосується права автора на твір № 4357 Україна. Комп'ютерна програма «Granulation Unit»/ А.Є. Артюхов, Я. Крмела, В.К, Ободяк, А.О. Горішняк. – опубл. 20.05.2019.

10. Ivaniia A.V., Artyukhov A.Y., Olkhovyk A.I. Hydrodynamic and thermodynamic conditions for obtaining a nanoporous structure of ammonium nitrate granules in vortex granulators / Springer Proceedings in Physics. – 2019. – 221. – pp. 257-268.

11. Artyukhov A.E., Artyukhova N.O. Technology and the main technological equipment of the process to obtain N4 HNO3 with Nanoporous Structure / Springer Proceedings in Physics. – 2019. – 221. – pp. 585-594.

12. Artyukhov A., Artyukhova N., Ostroha R., Yukhymenko M. Bocko J., Krmela J. Convective drying in the multistage shelf dryers: theoretical bases and practical implementation / Drying Unit Operations. – IntechOpen, UK, 2019. – pp. 140-163.

13. Artyukhova N.O., Krmela J. Nanoporous structure of the ammonium nitrate granules at the final drying: The effect of the dryer operation mode / Journal of Nano- and Electronic Physics. – 2019. – 11(4). – 04006-1-04006-4.